PEROVSKITE SOLAR CELLS AND THEIR TYPES

Muhammad Sikandar Subhani

Department of Chemistry, Bachelors, Riphah International University, Faisalabad (38000), Pakistan

Arooj Fatima

Department of Chemistry, Bachelors, Riphah International University, Faisalabad (38000), Pakistan

Aneeza Kokab

Department of Chemistry, Mphil Scholar, University of Okara (56300), Pakistan

Ayesha Riaz

Department of Chemistry, Assistant Professor, Riphah International University, Faisalabad (38000), Pakistan

Sana Mubashar

Department of Chemistry, Mphil Scholar, University of Okara (56300), Pakistan

Corresponding author: Sikandarsubhani884@gmail.com

Article Info

Abstract

Perovskite photovoltaic compartments have garnered momentous consideration in photovoltaics owing to their easy manufacturing process and high efficiency. The optoelectronic properties of perovskite solar cells (PSCs), made from halide and diverse-halide materials, are exceptional. Perovskite structures exhibit remarkable stability despite a wide band gap and minimal charge transfer. Some advantages of perovskite solar cells are; high efficiency, low cost, rapid manufacturing, flexibility, energy payback time, sustainability, etc. To address these challenges, multidimensional perovskite materials are utilized to achieve long-term stability and good performance. Recent advancements in low-temperature synthesis methods and improved contact and electrode components have resulted in PSCs surpassing an efficiency of 25%. Perovskites' characteristics can also be enhanced by altering their elemental makeup. The light-harvesting perovskite material, the electron-transporting layer (ETL), the transparent conductive oxide (TCO) film, the hole-transporting layer (HTL), and the metal contact material. The most fantastic and popular perovskite material for sunny collecting at the moment is MAPbI3. Compared to the conventional MAPbI3 perovskite, additional perovskite substances, for example, assorted halide-assorted cation, hybrid cation, and hybrid halide, are drawing more interest. This paper mainly discussed metal-based PSCs, non-metal-based PSCs, and polymer-based PSCs. Moreover, there has been a significant focus on the constancy and production concerns that boundary the commercialization and modularization of perovskite solar cubicles.

Keywords: *Perovskite solar cells; Photovoltaic technology; Efficiency enhancement; Hybrid materials; Stability challenges; Device architecture.*

Introduction

One of the most optimistic new solar-powered technologies is PSCs, which display exceptional supremacy adaptation efficacy through an easy, affordable solution-process technique. PSCs are a desirable alternative for standalone solar modules or as sub-cells for highly efficient perovskite-silicon photovoltaic cells because their certified proficiency increased to 25.2% in 2020.[1]. Due to their excellent photoelectric conversion efficiency, high absorption coefficient, variable band gap, wide carrier diffusion lengths, and comparably inexpensive material costs, inorganic-organic perovskite materials are fascinating and much considered for application in PSCs [2]. Significantly, the usage of halide perovskites in light-emitting diodes and energy conversion being studied (LEDs) [3], inexpensive transistors[4], as well as very effective photodetectors [5]. Due to their excellent band alignments, mixed-halide perovskites solar cells displayed significant PCEs. [6], dazzling carrier mobility and absorption coefficients [7], diffusion times[8], as well as low exciting binding energies[9]. Other exceptional qualities, including solid luminescence and low-temperature solution process ability, aid the development of perovskite materials. [10].

As the worldwide inhabitants extended day by day, so did universal power depletion. Climatic complications are fetched by using fewer remains gases and other non-renewable energy bases, promoting renewable energy implementation.[11]. Recently, numerous approaches, including solar architecture [12], solar energy[13], artificial photosynthesis [14], photovoltaic [15], water splitting during photo-catalysis [16], etc. erected to capture solar energy. A photovoltaic device known as a solar cell generates electricity using solar energy. Photovoltaic segments are frequently separated into three categories. Solar cells built on wafers make up the first era, photovoltaic cells based on thin films make up the second, along with biological structures make up the third. The usage of primary- and secondary-generation solar compartments has been impeded by their huge price, difficult manufacturing techniques, and adverse environmental impacts. As a result, scientists are looking for new, reasonably priced, and environmentally friendly solar cell materials. Polycrystalline silicon and Single-crystalline silicon photovoltaic cells are two different types of solar cells that have been used so far (c-Si cells) [17], CIGS photovoltaic panels[18], groups based on CdTe [19], solar cells with quantum dot sensitivities [20] as well as perovskite solar cells [21] have been documented.

Carbon is a terrific component with an extensive assortment of allotropes and bond conformations. For instance, fullerene (C60) has 60 particles systematized in a globular nanoparticle arrangement. Carbon nanotubes (CNTs) are a linear shape, whereas graphene is a sheet of carbon atoms one layer thick. Carbon black, activated carbon, and graphite all have typical three-dimensional configurations. These carbon complexes display excellent electrical, optical, chemical, and physical capabilities in each design.[22]. Due to its high bandgap, amorphous carbon is an antireflective sheet in transparent silicon photovoltaic cells of the first group [23]. The electrode material of thin-film solar compartments of the second type is carbon-based [24]. Bringing together the benefits of solar cells of the first and second generations, affordable and very effective solar cells of the third generation, such as dye-sensitized photovoltaic cubicles, carbon-based/biological solar cells, perovskite photovoltaic compartments, and others [25], were growing in popularity as a research topic recently. PSCs, a brand-new variety of third-generation solar cells, have undergone substantial development over the past ten years. PSCs could be manufactured in large quantities and later contribute to the production of photovoltaic vitality in the future because they are highly efficient in converting energy (PCE) and simple manufacturing [26].

The excellent concert is attributable to the favorable optoelectronic characteristics of the LHPs, including their ambipolar transportation properties, large transport movements, prolonged equilibrium carrier propagation widths, significant absorption coefficients, variable spectrum gaps, and low exciting binding strength [27]. The LHP has a structure of ABX_3, where a halide anion is X like Br, I, or Cl, and the cation

A is organic and inorganic like formamidinium (FA), methyl ammonium (MA), or Cs [28]. Although the PCE of perovskite photovoltaic compartments has significantly enhanced, unresolved scale-up and commercialization-related challenges exist. The search is currently on for long-term stable PSCs [29]. Similar or occasionally even better electrical as well as optical characteristics, for example, smaller photosensitive band gaps as well as higher charge transporter mobilities, are displayed by Sn-based perovskites [30]. Sn is a little-toxic component, and when exposed to air, Sn^{2+} breaks down to the environmentally beneficial compound SnO_2. In light of this, Perovskite absorbers made of Sn show promise for creating highly efficient Perovskite solar cells without pb [31]. This article will provide an update on current perovskite research photovoltaic compartments; in particular, we have concentrated on perovskite solar cells created on metal-based, non-metal-based, and polymer-based and their applications.

A photovoltaic compartment, also called a solar framework, is a piece of electronic apparatus that uses the solar power consequence, a chemical or physical process that transforms light energy into current [32]. A photoelectric cell is a device whose electric properties, for example, voltage, resistance, or recent variation when light is present. The foundation of photovoltaic segments is called solar cells or solar panels. Regardless of the source, sunshine, or manufactured light, photovoltaic cells are referred to as solar. They can measure the light intensity, operate as a photodetector, and detect light or other electromagnetic waves in the visual range (for instance, infrared sensors). Various categories of photovoltaic compartments exist as; photovoltaic cubicles made of buried contact, cadmium telluride (CdTe), copper indium gallium selenide (CI (G) S), bio hybrid, dye-sensitive solar cells (DSSC), gallium arsenide germanium (GaAs), nanocrystal, amalgam, polymer, quantum dot, and perovskite. We focus on describing the Perovskite photovoltaic cell in this article [32].

2: Perovskite photovoltaic-compartments

Typically, the essential qualities of the excessive absorption coefficient of perovskite solar cells are what account for their photovoltaic performance [6], a variable band gap [33], lengthy carrier diffusion [34], ability to transfer ambipolar particles [2] likewise carrier mobility [8]. In particular, the best choices for developing organic-inorganic hybrid-perovskite (OHIP) materials include compelling and inexpensive solar cells. The OHIP material was first demonstrated by Mitzi and colleagues for use in applications for transistors and light-producing diodes during the 1990s using the ABX_3 is a chemical formula, where A stands for a carbon-based cation group like Cs^+, formamidine (FA^+, $CH_3CH_2NH_3^+$) and Methyl Ammonium (MA^+, $CH_3NH_3^+$), where B denotes an inorganic positive ion assembly such as Sn^{2+} or Pb^{2+}. X represents halide particles such as Cl, Br, I, etc., [35]. In addition, compared to natural-inorganic composite, perovskites exhibit remarkable photonic and electrical features as natural and artificial semiconductor devices. These OHIP resources also have a broad Bohr radius range [36], mediocre unalterable power [37], increased insulator persistence [38], and elevated transporter dispersion length or velocity [39] paired with exceptional luminescence absorption capabilities. Ascribed to these assistances, OHIP ingredients are designed to the maximum of the list of challengers for manufacturing cheap, extremely active solar cells. In perovskite photovoltaic compartments, the HTL and ETL are often separated by an absorber layer, such as $CH_3NH_3PbX_3$ (HTL). When visible to light, the perovskite absorber familiarizes n-type and p-type electrons and hole carriers that carry ingredients to create bearers of unrestricted charge. The electrons moved through the mesoporous film and an outside route before being received at the cathode. Furthermore, the tarnished perovskite is returned and facilitated to influence ground state by the concise serving of the hole-conveying substantial. As a result, the opposite is diffused by the HTM gap way of an electrode recombines using an electron to produce the current in the end. The current generation is dependent on the perovskite material's thickness [40]. Figure 1 depicts perovskite solar cells' levels of power and the charge-allocation procedure [41].
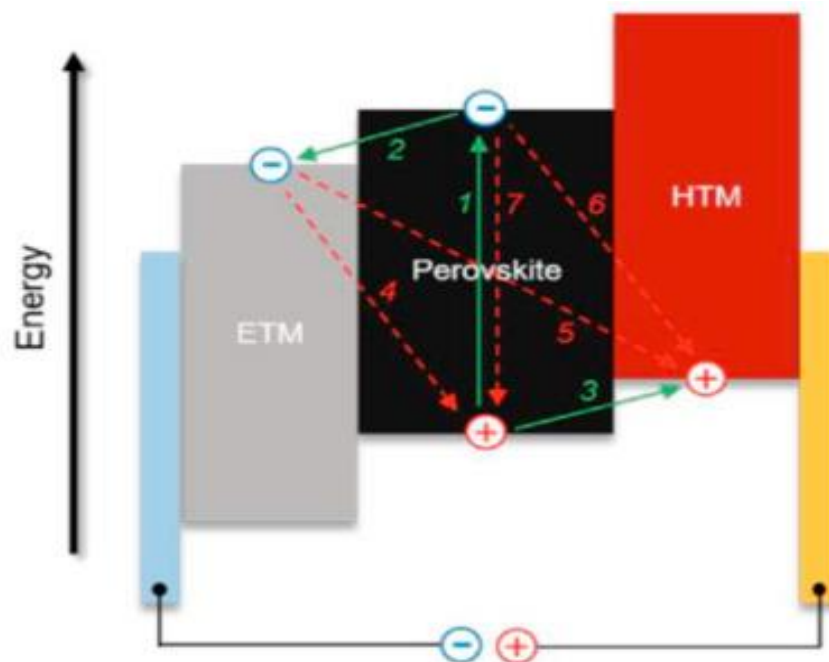
Figure 1: Perovskite photovoltaic compartments energy levels and charge-transfer mechanism [41].

Miyasaka and colleagues first used 2009 applications of perovskite materials in solar cells [42]. Solar cells with dye-sensitization (DSSC), which exhibit a PCE of 3.81%, used $CH_3NH_3PbX_3$ as a sensitizer. According to later investigations, OHIP ingredients are predominantly fascinating opportunities for solar compartment submissions. In addition, the abundance of the OHIPs' precursor components and straightforward synthesis methods such as vacuum-deposition [43], processing of atmospheric solutions [44] etc., were positioned. Several unexpected breakthroughs are made quickly, with the PCE increasing to 23.3% [45]. Additionally, ETL is essential to developing perovskite solar compartments [46]. ETL is a colloidal tinny film of SnO_2 used in classic perovskite photovoltaic cells. [47], titanium dioxide TiO_2 [48], and the mesoporous systems of ZnO [49], which have thick grain boundaries and weak interface recombination [50]. Specifically, vacancies in oxygen and trap-assisted constellate caused spontaneous defects in semiconductor ETL [51]. Researchers developed many addresses to these issues, and ingredients for ETL in perovskite photovoltaic cells (individual crystalline) are needed. This viewpoint considers dichalcogenides of transition metals like WS_2, TiS_2, MoS_2, etc., to be nanosheets or atom-thick materials [52] and has a lot of possibilities to be rummage-sale as ETL content. Considering that atom-thick, single-quartz nanosheets are essentially imperfection-permitted [53].

Additionally, the thin construction allows for quick delivery to the electrode of charge carriers [54]. Because of its excellent carrier transference ability and low deception density, MoS_2 is a well-liked ETL [55]. Due to its ambipolarity, it can occasionally be used as HTL [56]. As a result of the increased electron mobility [57] and many different nanostructured morphologies [58], ZnO might potentially be an excellent photovoltaic compartment application of preference because of its versatility or several expanding procedures [59]. The performance of a perovskite photovoltaic framework is well known, dependent on the transparent nature or exterior shape of the perovskite layer of regulating.

Additionally, the structure (particle shape and surface smoothness) of the active phase of a perovskite prepared with an appropriate solvent can significantly affect the performance of photovoltaic cells.

pg. 48

Ahmadi et al. latterly developed a cost-effective ultrasonic bath method [60] for perovskite solar cells to build ETL; Three different solvents made of zinc oxide nanoparticles are used:2-methoxy ethanol (2 ME), ethanol, and isopropyl alcohol (IPA). According to the findings of investigations into the structure, morphology, and device performance, the layer of ZnO produced utilizing as the solvent, 2 ME displays the best potentials of all those arranged. Additionally, ZnO (2 ME) as the ETL and methyl ammonium lead iodide (MAPbI$_3$) as the outermost perovskite layer are used in a perovskite photovoltaic cell with a high PCE of 22%. This is due to the lowest at the ZnO (2 ME)/MAPbI$_3$ interface; fault density, bigger grain sizes, and excellent MAPbI$_3$ surface coverage were reported. ZnO photovoltaic compartments are thus a perfect choice for photovoltaic cell uses. Transmittance is significant in photovoltaic cells; ZnSnO (ZTO) can also be utilized as an ETL. The transmission of charge carriers often depends heavily on the oxygen vacancies in ZTO. The quantity of oxygen vacancies in ZTO is a severe problem as well. To remedy this, Miao et al. [61], by creating based on ZTO solar cells with Si-doped at various doping concentrations, oxygen vacancies' effects on ZTO were established.

2.1: Perovskite materials

Perovskite solar cells continue to advance, which is impressive given the development of novel cell ingredients and the most current steps taken to understand the operating principles of perovskite devices better. The electrical and optical characteristics of the final device are strongly influenced by the two designs regarding the perovskite solar cell as a whole and the material selection. Perovskites' characteristics can also be improved by altering their elemental makeup. The light-harvesting perovskite material, the transparent conductive oxide (TCO) film, the hole-transporting layer (HTL), the electron-transporting layer (ETL), and the metal contact material are the five groups into which the components can be used perovskite photovoltaic compartments divided. The significant structures that have influenced the current exploration of perovskite-type photovoltaic compartments are covered in the following subsections.

As previously mentioned, a halide ion, a monovalent cation, and a divalent cation are commonly present in perovskites used for light harvesting. The most excellent and popular perovskite material for sunny collecting at the moment is MAPbI$_3$. Compared to the conventional MAPbI$_3$ perovskite, additional perovskite substances, for example, assorted halide-assorted cation, hybrid cation, and hybrid halide, are drawing more interest. Researchers are now looking for alternatives to Pb to evade the intrinsic harmfulness of lead. The three subcategories that follow discuss current research and studies into a variety of ingredients [62].

2.1.1: Lead halide perovskites

The performance of PSCs can be enhanced by altering monovalent cations. There is a quest for alternative efficient substances to methyl ammonium (MA) in MAPbI$_3$ due to its inadequate energy gap and problems caused by long-standing constancy. However, MAPbI$_3$ is a perovskite solar cell's comprehensively employed light buckler [63]. Even though the observed band holes of MAPbI$_3$ are between 1.50 to 1.61 eV, the ideal energy gap for an isolated junction photovoltaic cell is 1.1 to 1.4 eV [64].

Manipulate inferior energy gap perovskites, whereas MAPbI$_3$ can increase the photovoltaic light-collecting proficiency of PSCs even more. A modified monovalent cation may alter the length and angle of the Pb-I bond in a lead halide-constructed perovskite, which may change the material's overall band structure [65]. The band gap is slightly reduced when the MA ion is swapped out for the somewhat larger organic formamidinium (FA) ion, going after MAPbI$_3$ 1.59 eV to FAPbI$_3$ 1.45-1.52 eV, which exists nearer to the ideal band hole of an isolated coupling photovoltaic cell and consequently, permits to extract

further light [66]. Also, Hanusch et al. demonstrated that FAPbI$_3$ is a more efficient heat balance than MAPbBr$_3$ or MAPbI$_3$, which is consistent with the investigations that a more significant positive ion at the A region of the ABX$_3$ formation could sustain the perovskite arrangement [67]. FAPbI$_3$ is capable of, however, elucidating into a single photoactive perovskite segment (red appearance) and the light-sensitive, non-perovskite hexagonal patch (yellow part) (black phase) [68], which is delicate to humidity and solvent contamination [69], resulting in stability problems.

On the other hand, as much as others stay within the liberality feature span, univalent positive ions can further be replaced with dead substances for additional enhancement. The tolerance factor for the common monovalent cations MA and FA and the immovable alkali alloys A = K, Li, Rb, Cs, and Na. According to the sufferance aspect diagram, CsPbI$_3$, FAPbI$_3$, and MAPbI$_3$ have a dark phase and fall between 0.8 and 1.0. The fixed range is unquestionably outside the Li-, Na-, and K-based perovskites, whereas RbPbI$_3$ is only marginally outside. Additionally, it can be observed that whereas RbPbI$_3$ stays yellow when heated, CsPbI$_3$ turns the film black. As a result, even though Rb has high oxidation stability, it cannot be employed in perovskites. However, CsPbI$_3$ has outstanding heat resistance; its band delay (1.73 eV) is not optimal for use in only-joint solar. At room temperature, it is unbalanced in the three-dimensional or pseudo-cubic stage [70]. Designing mixed cations/ halide perovskite compounds is essential to achieving more excellent competencies and long-standing structural and heat constancy because of the drawbacks of uncontaminated single positive ion-solitary halide perovskite composites. A tiny amount of MA and FA in perovskites shows superior photoactive black phase crystallization and, as a result, higher thermal and physical permanency than pure FA or MA perovskites, according to double cation MA/FA perovskites [69]. Recently, Prochowicz et al. were able to achieve 23.7 mAcm^{-2} substantial short-circuit charge density (JSC) with a PCE of 14.98%, demonstrating suggesting the 25% addition injecting MAI into the combination of processes maintained the FAPbI$_3$ the dark portion [72].

Organic-inorganic double-cation perovskites and positive ion-based natural MA/FA mixture Perovskites were also investigated. Choi et al. revealed that increasing the variation in energy within the perovskites, the valence region, and PCBM's lowest level of unoccupied molecular orbital (LUMO) led to a 40 % increase in device efficiency when 10 percent doping in the Cs MAPbI$_3$ structure of perovskite [73]. Lee et al. discovered that FA 0.9Cs 0.1 PbI$_3$ had significantly better photo and moisture stability than pristine FAPbI$_3$ [74].

Similar to how MA and FA can be combined, a minor portion of MA or FA can be swapped out for Cs to enhance the ocular and charged premises and boost manoeuvre production. The use of Cs to investigate more intricate cation combinations, such as Cs/MA/FA, was done to increase stability and device performance. Compared to MA/FA double-cation perovskites, the three-layered-cation (Cs/MA/FA)-based PSCs exhibit higher repeatability and current stability. Their stabilized PCE is 21.1% [70]. The cubic PbI$_2$ and the photo-indolent hexangular δ-segment of FAPbI$_3$ can be entirely dissipated by adding Cs to the MA/FA cation combination. Additionally, enumerating Cs in different amounts (5, 15, and 10%) led to a 10 nm shift in blue in the photoluminescence (PL) bands or captivation and a smaller cationic radius, which allowed the endurance aspect to lean further towards a three-dimensional framework assembly and increased the entropy stability of the black perovskite stage at ambient temperature [70] Fig. 3 displays these findings. This vital breakthrough makes it possible to investigate using other erosion-steady antacid alloys, including K, Rb, Li, and Na, as univalent positive ions for perovskites.

To investigate different univalent positive ions, Saliba et al. Rb was recently added to a photoactive perovskite stage employing formulations with numerous cations (RbCsMAFA) [71]. They discovered that the uncontaminated RbPbI$_3$ molecule is not appropriate for use in perovskite photovoltaic compartments

pg. 50

because of its intrinsic oxidation instability; Rb container be incorporated into various positive ion-constructed perovskites due to Rb's capacity to maintain the FA perovskite's black phase. When compared to formerly investigated divalent combination-constructed perovskites like CsMAFA and CsFA, they found a variety of cationic combinations with consistent device performances; RbFA, RbMAFA, RbCsFA, and RbCsMAFA are a few examples, from five percent RbCsMAFA Rb in, they achieved a stable competency of up to 21.6 % [71]. These findings made using different inorganic cations and various organic-inorganic cation combinations in perovskite photovoltaic compartments possible. The optoelectronic characteristics of perovskites can be tuned via halogen ion replacement or mixing. Large single crystals of all three lead halide perovskites, $MAPbI_3$, $MAPbCl_3$, and $MAPbBr_3$, have been produced, and iodine identified in lead halide perovskite ($MAPbI_3$) assembly may be swapped using such as chlorine or bromine.

Liu et al. investigated how the halogen anions affected the optical properties of $MAPbX_3$ (X = Cl, Br, I), including its band gap spectrum of absorption and photoluminescence bands [76]. They determined that the halide substitution between I, Br, and Cl caused a considerable shift in absorbance. For a single crystal, the band gap concerning I, Cl, and I perovskite is 2.97, 2.24, and 1.53 eV, indicating that the band gap energy decreases as the halide's ionic size increases [76]. Furthermore, they are favorable for use in solar cells because of the lesser PL peak values relative to absorption development [76].

Each perovskite structure has advantages from a photovoltaic standpoint. For instance, $MAPbCl_3$ is preferable for light-emitting components, whereas $MAPbI_3$ and $MAPbBr_3$ are more appropriate for single-band slit absorbers and dual uses [77]. Halides can, however, be used with perovskites to produce other advantageous results, such as improved band gap tuning, transport carriers, and stability. Lee et al. discovered that during processing in the air, hybrid halide perovskite $MAPb(I_{1-X}Cl_X)_3$ is more durable than $MAPbI_3$ [78]. Noh et al. It was proven that adding Br to $MAPbI_3$ conversion rate is 20-29 percent considerably improved the consistency of the generated photovoltaic segments while maintaining cell proficiency [33]. Furthermore, compared to $MAPbI_3$, $MAPb(I_{1-X}Cl_X)_3$ had more extraordinary electron-hole dispersion lengths. Both diverse halide perovskites, $MAPb(I_{1-X}Br_x)_3$ and $MAPb(Br_{1-X}Cl_X)_3$, experienced an increase in carrier mobility and carrier recombination rates. [79]. Mixed (I, Cl) perovskite formation becomes intricate when temperatures below 625 K. In contrast, the construction of diverse (Cl, Br) and (Br, I) perovskite is easily achieved at room temperature [80]. The I/Br-halide mixture holds incredible promise regarding overall performance.

By harnessing the benefits of different elements and mitigating their limitations, it is possible to fabricate a perovskite solar cell that incorporates both cations and halides. Jeon et al. conducted a comparison between various arrangements for example; $MAPbI_3$, $FAPbI_3$, and $MAPb (I_{0.85}Br_{0.15})_3$, and found that $(FAPbI_3)_{0.85} (MAPbBr_3)_{0.15}$ offers numerous advantages [69]. However, research on controlling various perovskite components' composition is ongoing. Jacobsson et al. They raised the PCE for a mixed perovskite solar cell featuring double cations and double halides up to 20.7%, demonstrating that a slight modification in the chemical composition significantly impacts the materials' characteristics as the device performance [81]. As mentioned earlier, researchers incorporate cations (triple, quadruple) into the mixed halide to increase the proficiency and solidity of perovskite [82].

Although lead toxicity continues to be a problem that limits commercialization attempts despite improvements in lead-based perovskites' efficiency over the past few years, it is also crucial to identify less toxic/non-toxic functional elements to substitute lead and boost the effectiveness and stability of perovskites from a toxicological and environmental standpoint. Sn, Ge, Cu, Sb, Bi, and Sr are a few other elements that have been the subject of extensive research because they may one day replace lead [83].

One of them, Sn-based perovskites (MASnI$_3$), has a maximum efficiency of 6% [84]. Sn-based perovskites can undergo oxidation, transitioning from Sn^{2+} to Sn^{4+}. As a result, they are prone to self-doping and structural instability, leading to rapid degradation upon exposure to ambient air. However, a significant focus has been recently on Pb-Sn binary perovskites due to their enhanced performance and reduced toxicity. Various efforts have been undertaken to regulate the natural configuration of both Pb and Sn and refine the production methods for optimal outcomes [85]; according to reports, the following advancements have allegedly resulted in remarkable reproducibility and a PCE of 15.08 % [86].

According to density-functional-theory (DFT) simulations, germanium (Ge) is a promising alternative for the divalent metal cation in the perovskite structure, suggesting it could effectively replace Pb. This computational screening indicates that Ge holds significant potential as a suitable candidate element [87]. Ge-based perovskites had previously failed to yield any significant breakthroughs. Still, a recent study by Krishnamoorthy et al. revealed Ge-based perovskite solar compartments attaining a determined PCE of only 0.20 %, along with notably weak open-circuit voltages [88]. Kopacic et al. also introduced bromide particles into the methylammonium germanium perovskite (MAGeI$_2$.7Br$_{0.3}$) to modify its composition. By employing a two-dimensional p-i-n device arrangement, they successfully attained a peak PCE of 0.57 % [89]. Moreover, researchers strive to utilize cations apart from group 14 elements to substitute lead. A recent achievement by Shai et al. involved the development of a binary Pb-Sr-based perovskite solar cell (PSC). By incorporating a small quantity of Sr (0.05) into the MASr$_a$Pb$_{1-a}$I$_{3-x}$Cl$_x$ crystal structure, they achieved an impressive(PCE of 16.3 % [90].

In addition to selecting the best material, acquiring a perovskite film of the highest calibre is crucial. Numerous firm-forming techniques, including spin coating, have been developed [91], doctor's knife [92], coat in a dip [93], die-slot layer [94], the act of applying paint using a spray technique [95], the process of printing using inkjet technology [96], deposition relying on vapour [97], etc. Spin coating is the most well-known and widely applied film-forming technique in producing perovskite solar cells on a lab scale. The advantages of this approach include the ability to create thin sheets with well-defined and homogeneous thicknesses [98]. However, huge-scale manufacturing of perovskite photovoltaic compartments is not suitable.

Additionally, the spin-covering procedure results in material waste, which raises the price of fabricating PSCs. In contrast, to spin coating, doctor blade processes provide simple and inexpensive film production with nearly little material waste [99]. However, this technique makes it challenging to regulate the film's thickness. Perovskite solar cells now feature slot-die coating [100]. By employing this technique, Qin et al. achieved a power conversion efficiency (PCE) of 14.7% using a dynamic range of 10 mm^2 [101]. However, using this technique to produce thin films is similarly challenging. Spray-coating technology reduces the cost of manufacturing PSCs on a broad scale, but the film quality suffers due to the technique's poor film consistency and stability [102]. Ink-jet production is an alternative or effective technique for forming highly controllable and precise thin films. Due to the minimal material waste generated during manufacture, this process is economical [96]. The spin-coating method can be considered one option for producing PSCs based on vacuum, while these non-vacuum-based methods provide an alternative approach. However, a drawback of these techniques that might impair the performance of PSC devices is their inability to control the surface morphology of perovskites [103].

2.2: Magnetron Sputtering

The unstructured metallic oxide films are generated complete the RF magnetron spattering method, which alters the silicon absorption. Furthermore, the confirmation of reduced oxygen vacancies compared to

silicon concentration was obtained by analyzing X-ray photoluminescence spectra (XPS). Again, the enhanced capability of SZTO for electronic extraction and transfer is achieved by eliminating oxygen vacancies. Utilizing the developed SZTO as an ETL, they successfully fabricated a perovskite solar cell that attained impressive performance metrics, including a maximum power conversion efficiency (PCE) of 13.4%, a short-circuit current (J_{OC}) of 21.6 mAcm^{-2}, an open-circuit voltage (V_{OC}) of 1.04 V, and a fill factor (FF) of 0.67.

Moreover, TiO_2-based photovoltaic cells exhibit a favorable PCE exceeding 20%. Nevertheless, when exposed to UV radiation, the TiO_2 ETL in n-i-p structured perovskite solar cells leads to instability and rapid deterioration of the short-circuit current density (J_{SC}) [104]. Many researchers have dedicated their efforts to tackling these challenges or protecting perovskite solar cells from degradation caused by exposure to ultraviolet (UV) light by using an interface layer between perovskite and TiO_2-ETL [105]. However, TiO_2 impacts the device's performance in the abovementioned methodologies. Hence, developing stable perovskite solar cells with improved efficiency becomes imperative. Numerous ETL materials with high resistance to UV radiation have garnered significant interest in this regard [106]. One material that stands out is $Mg_xZn_{1-x}O$ (MZO), which can potentially serve as an effective ETL material in perovskite solar cells. MZO exhibits excellent stability when exposed to ultraviolet radiation, thanks to its high electron mobility and conduction band with no lower limit [107]. Following this, Han et al. [108] recently the remarkable durability of the perovskite solar cell based on MZO was unveiled in a study. The researchers highlighted that MZO demonstrates enhanced carrier mobility and conduction mechanisms in comparison to TiO_2. This attribute effectively prevents the formation of charges at the interface of MZO and perovskite, thereby enhancing the inter-material transfer between the two substances.

Furthermore, a device based on MZO was developed, exhibiting exceptional performance with an impressive competency of 19.57 percent and an extended open route current of 1.11 V in its optimal state. Moreover, even after a year of exposure to room temperature, 40 to 80% relative humidity, and 8 hours of UV revelation, the suggested expedient maintains a remarkable 76% of its initial J_{SC}. The TiO_2-based device only retains 12% of the primary J_{SC} below similar environmental circumstances. The superior UV stability of the manufactured expedient can be credited to the lower density of electron deception states in the MZO-ETL (electron transport layer). This can be attributed to MZO-zinc-interstitial ETL and oxygen-position spots, which actively prevent degradation of the perovskite layer when visible to UV brightness. Consequently, the proposed MZO-ETL holds excellent potential for producing durable perovskite solar cells resistant to UV radiation.

2.3: Enhance the Conductivity of the Electron Transport Layer

To increase the ETL layer's conductivity, Teimouri et al. [108] showed how lithium (Li) doping affected TiO_2. They employed ultra-sonication to produce films of Li-doped TiO_2, aiming to enhance conductivity and minimize solar power loss in a liquid state. Consequently, perovskite solar cells utilizing c-TiO_2 open a new pathway for producing more efficient perovskite solar cells at lower temperatures. Figure 2 depicts a schematic for perovskite solar cells made of c-TiO_2 [109].

Using a straightforward sintering process, Zhang et al. [110] constructed layers of mesoporous TiO_2 with $MgTiO_3$ coating at various treatment concentrations for solar cell applications. Applying the generated scaffolds as outer layers resulted in a significant enhancement in the photovoltaic capabilities. The presence of the $MgTiO_3$ shell serves as an effective barrier, preventing charge recombination at the interface of $MAPbI_3$ and TiO_2. Furthermore, including $MgTiO_3$ improves the crystal structure of $MAPbI_3$, which is crucial for producing superior perovskite films. By utilizing an optimal treatment concentration

of 0.10 M, the PSCs achieve a maximum PCE of 10.39%. Furthermore, even after being stored in the air for 1008 hours under typical humidity conditions, the perovskite device holds 88.35 percent of its primary PCE. Applying MgTiO$_3$-covered TiO$_2$ mesoporous framework coatings demonstrates their suitability as materials for next-generation photovoltaic systems, thanks to their long-term firmness, more PCE, and ease of production.
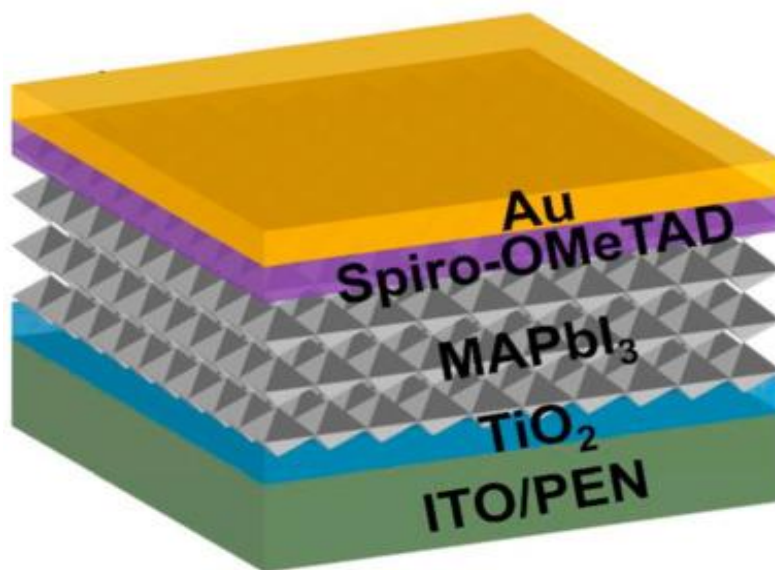
Figure 2: Perovskite solar cells with a c-TiO$_2$ base are seen schematically [109].

Moreover, the exceptional chemical stability, inclusive bandgap, high electron movement, and anti-reflective properties of indium oxide (In$_2$O$_3$) thin films make them highly promising ETL ingredients in perovskite solar cubicles [111]. Former works demonstrate that the hygroscopic nature of In^{3+} leads to the formation of flawed crashes, pinholes, and structures. This results from the interaction between In^{3+} cations and water molecules during the sample synthesis [112]. In the realm of solar cells, In$_2$O$_3$ may not emerge as the primary candidate for the ETL due to certain limitations. It is highly desirable to obtain flawless In$_2$O$_3$ to enhance the routine of solar devices. Notably, this marks the first instance where this aspect has been explored, Zhang et al. [112] confirmed the construction of condensed In$_2$O$_3$ sheets using a remarkably stable indium precursor solution. These films can be processed at low temperatures and effectively function as a reliable ETL in PSCs. The indium antecedent exhibits exceptional durability in ethanol and possesses a water content of 0.2 percent.

To inhibit indium hydrolysis, the solution is supplemented with acetyl acetone (acacH), a chelation ligand [113]. These factors contribute to forming an In$_2$O$_3$ film under low-temperature conditions of 200 °C and relative humidity levels ranging from 40 to 50%. The impact of acetyl acetone as a chelation ligand on the stability of indium-precursor solutions was schematically depicted in figure 3 [112]. Applying an In$_2$O$_3$-film as an ETL significantly enhances electron extraction at the ETL/perovskite boundary and enables charge transmission. Consequently, the PCE of perovskite solar cells treated with air and utilizing a compact In$_2$O$_3$ film reaches 13.97%, whereas the PCE for cells incorporating a new In$_2$O$_3$ film is 9.81%. The proposed perovskite solar cell, which employs an indium-based material, demonstrates remarkable extensive solidity by absorbent 94 percent of its PCE later 31 days of packing and achieving a high PCE. These results collectively indicate that the utilization of In$_2$O$_3$ films as ETL significantly enhances both the stability and PCE of perovskite solar cells when subjected to air processing.

pg. 54
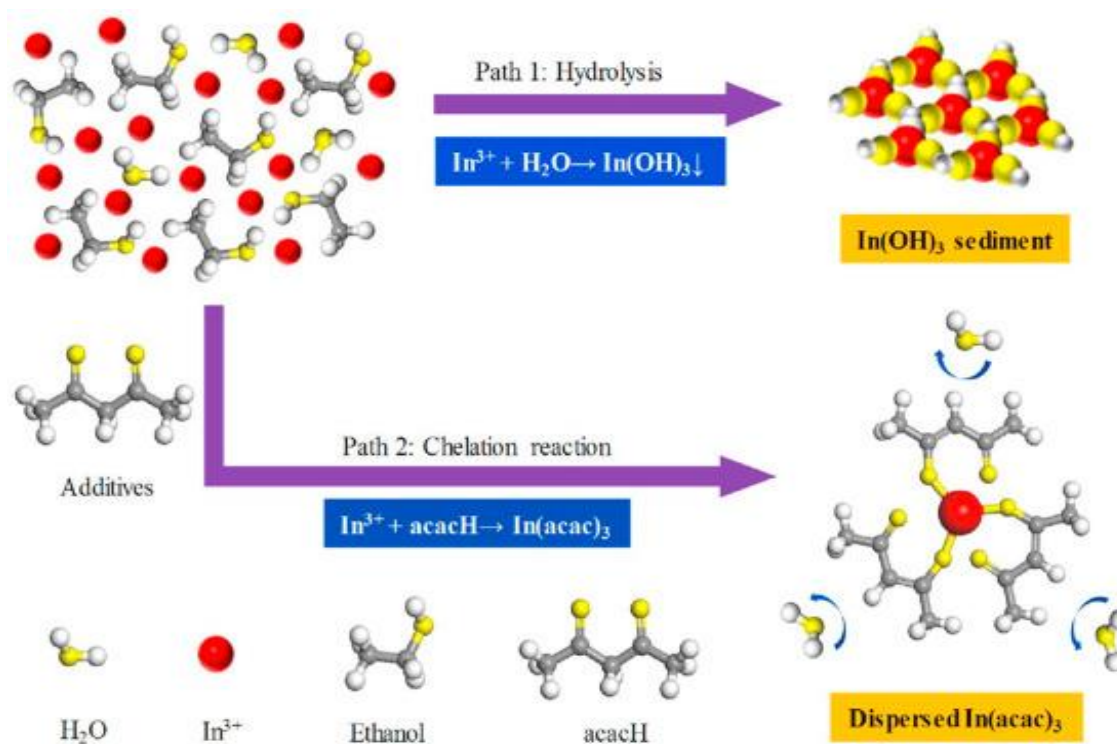
Figure 3: A schematic representation illustrates the constancy of indium-antecedent results, both with and deprived of the inclusion of acetyl acetone [112].

Tseng et al. [114] described an innovative approach for enhancing the PCE of PSCs. This approach focuses on modifying the structure, interface, and charge concentration of the hetero-structure composed of $Cu_2O/MAPbI_3/SiO_2$. Consequently, this device attained the maximum PCE of 18.4% with its improved VOC. As a result, various inorganic substances such as Cu_2O, SiO_2, and others hold promise as viable candidates for integration into perovskite solar cells.

2.4: Perovskite crystal structure

The material known as perovskite, discovered in the Russian Ural Mountains in 1839, holds great potential as a light-absorbing substance in developing advanced solar cells. Credit for its naming goes to the Russian mineralogist L.A. Perovski [115]. Perovskite, or calcium titanium oxide, is an inert with the natural formula $CaTiO_3$. It belongs to a group of substances with similar chemical composition to $CaTiO_3$ (ABX_3). In the ABX_3 structure, as illustrated in Figure 8a, the cubic space is filled by a sizeable monovalent cation A, a negligible bivalent metal positive ion B that occupies octahedral sites and an anion X. The anion X is naturally a halogen but can also be nitrogen, oxygen, or carbon. Cations A and B are commonly bivalent and tetravalent in this structure when the anion is O^{2-} [116]. Nevertheless, when a halogen takes on the role of an anion within a perovskite morphology, it gives rise to univalent and bivalent cations in the A and B spots, correspondingly [116].

pg. 55
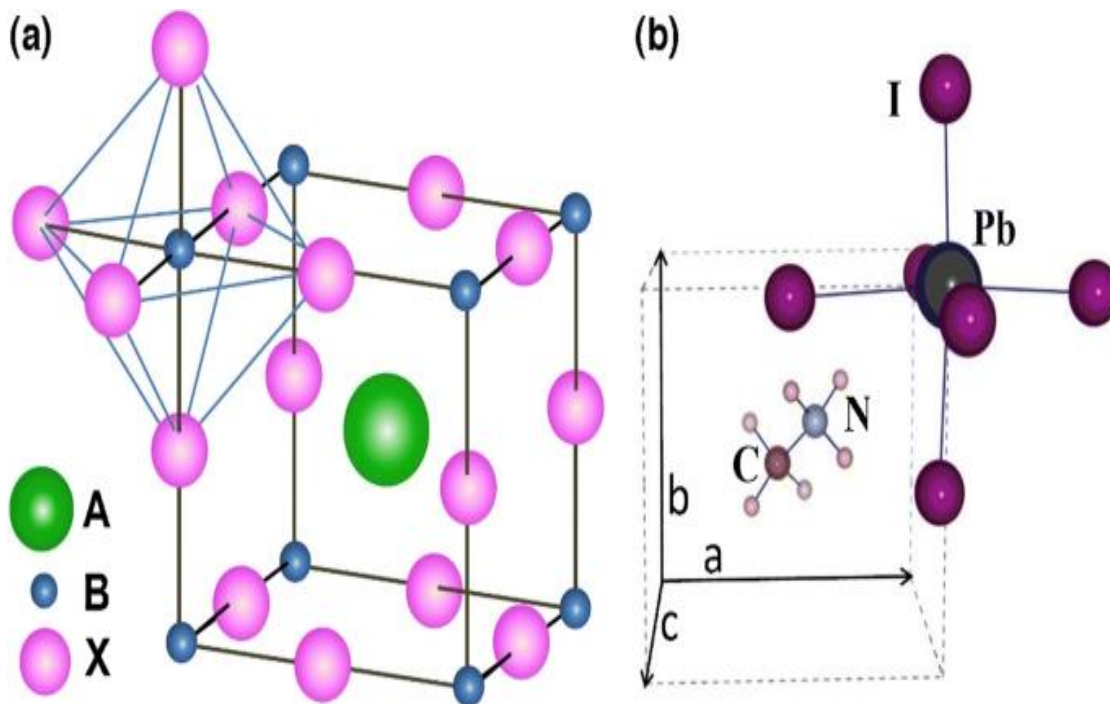
Figure 4: (a) Shows a larger ABX₃ perovskite structure in A cation occupying the cub octahedral site and BX₆ octahedral cation. (b) The cubic MAPbI₃ perovskite's unit cell [116].

Table 1: Specific PSCs photovoltaic parameters (RH 40 percent) [117].

Additive	Jsc (mA/cm²)	Voc (V)	FF	PCE (%)
Unspoiled / Primitive	18.02	0.84	0.51	7.71
PVP at 2% weight	18.14	0.85	0.54	8.34
PEG at 0.5 weight % + PVP at 1.5 weight percent	19.81	0.90	0.54	9.62
PEG 1 weight % + PVP 1 weight percent	19.13	0.90	0.54	9.23
PEG 1.5 weight percent + PVP 0.5 weight %	18.25	0.89	0.54	8.76
PEG 2.5 wt%	18.63	0.86	0.50	8.07

PSCs commonly utilize MAPbI₃, FAPbBr₃, and CsPbCl₃, which are representative ABX₃ light-absorbing compounds [118]. The arrangement of ions in the perovskite crystal structure of a unit cell is influenced by tolerance factor (t), pressure (P), and temperature (T). The mineral perfection can be enhanced by adopting the orthorhombic, tetragonal, and cubic structures for the perovskite crystal [119]. In perovskite

crystal structures, stability is predicted by the tolerance factor (t). In an ideal perovskite three-dimensional assembly, the value of the (t) feature is 1.0 but ranges from 0.8 to 1.0 in a less-than-ideal scenario. A low (t) factor produces less organized perovskite crystal formations like orthorhombic and tetragonal [120]. Similarly, when MA^+ and Cs^+ are used to create multi-cation perovskite alloys, the resulting materials exhibit comparable characteristics to those solely containing FA^+. In light of this, perovskites, including FA^+, may be said to be more stable than those containing only MA^+ and Cs^+ [121].

Table 2: Specific PbI₂ precursor solution composition parameters [117].

CH₃NH₃PbI₃ feature	PEG Content (weight percent)	PVP Content (weight percent)
Primitive / Unspoiled	0	0
PEG preservative	2.5	0
PVP/PEG stabilizer	0.5	1.5
PVP additive	0	2
PVP/PEG stabilizer	1.5	0.5
PVP/PEG additive	1	1

2.5: Working Principle of PSCs

The fundamental processes involved in the functioning of solar cells include light absorption, charge separation, charge transport, and charge collection. Appropriate light harvesters must be chosen to establish these processes effectively, and their optoelectronic characteristics must be studied. For example, when the light harvester is an intrinsic semiconductor, a p-i-n intersection becomes necessary. On the other hand, if the bright gatherer possesses n-type or p-type properties, a p-n meeting is required because n- or p-categories can transfer electrons or holes to the light harvester. Due to their balanced charge transport properties, organometallic perovskite materials can be employed in p-i-n and p-n connection types [122]. Electron and hole transport features were documented for $CH_3NH_3PbI_3$, synthesized through various methods involving a mixture of $CH_3NH_3I + PbI_2$ and another assortment of $3CH_3NH_3I + PbCl_2$. Irrespective of the preparation method, the X-ray diffraction patterns consistently showed indexing as tetragonal $CH_3NH_3PbI_3$ [122]. Due to the complex structure of the perovskite environment, there is still a lack of complete understanding among researchers regarding the generation and accumulation of charges in PSCs.

Consequently, the description of features in perovskite solar cells continues to rely on the same principle employed for silicon solar cells [123]. The perovskite layer collects photons and excitons when sunlight hits it. When the excitons are separated, the exons can generate both electrons and holes because of the differences in the necessary vitalities of the excitons in the perovskite material. Exciton departure occurs at the boundary among the charge and hole transport layers. Simultaneously, the holes are directed toward the holes transference layer and subsequently shifted to the cathode, generally composed of metal figure 5. On the other hand, the electrons are detached from the dumps and introduced into the ETL, naturally progressing toward the anode made of Fluorine-doped Tin Oxide (FTO) [124]. The hostage electrode is linked to an exterior route to produce a current, whereas the metallic electrode accumulates electrons and holes.
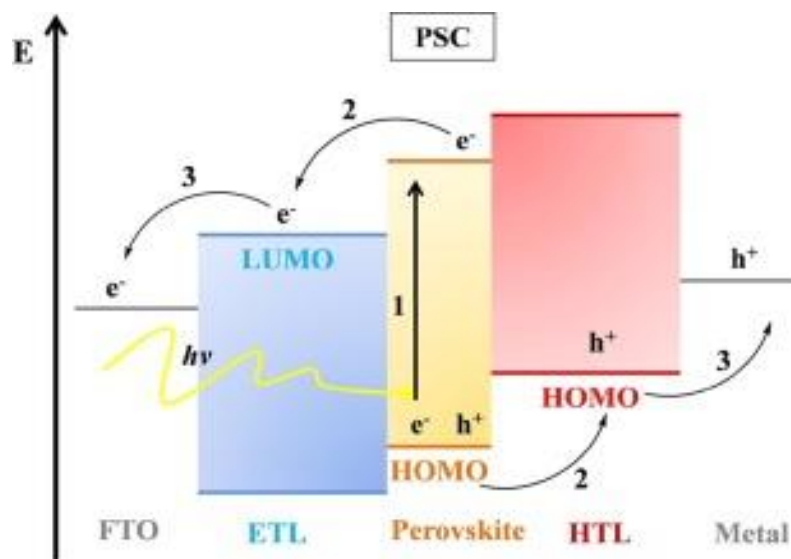
Figure 5: Show the Principles and working of PSCs [102].

3: Types of Perovskite Solar Cells

3.1: Metal-based PSCs

Lead halide perovskites, with the universal method $APbX_3$ (where A represents Cs^+, methyl ammonium (MA^+), formamidinium (FA^+), or their mixtures; and X represents I^-, Br^-, or combinations thereof), have emerged as a remarkable semi conductive material utilized in solar cells and various optoelectronic submissions in recent years [120]. Recently, PSCs achieved a verified (PCE) power conversion efficiency of 25.2 percent [125]; Perovskite solar cells demonstrate a level of routine that is on par with silicon solar cubicles. Nevertheless, there are substantial concerns regarding the practical implementation of PSCs, primarily stemming from toxic lead in perovskite materials. To create environmentally sustainable lead-free PSCs, replacing lead with tin is one viable technique [126, 127]. Due to its classification as an assembly of 14 atoms, tin-based perovskites possess optoelectronic capabilities on par with their lead-based counterparts. Additional benefits include an ideal band gap, reduced exciting necessary power, and enhanced transporter flexibility. As a result, creating high-performing tin-based PSCs has much potential, and further work is being done to show this potential [128, 129].

3.1.1: Metal-based Structural properties

It has been reported that many tin-based perovskites, including $CsSnI_3$, $MASnI_3$, and $FASnI_3$, can be used to create lead-free PSCs. $FASnI_3$ was the one that received the most attention because it typically displayed the best device performance and reproducibility [128]. Early investigations revealed that obtaining semiconductor tin-based perovskite films proved challenging due to the tin oxidation-induced "self-doping" phenomenon. Consequently, the repeatability of the solar cells was found to be relatively low [80, 130]. Several approaches have been put up to address this issue, including film morphology control [131], adding a lowering environment to promote the development of films [132], subsequently, the perovskite precursor solution undergoes the inclusion of tin halide, either SnF_2 or $SnCl_2$ [133, 134]. Finally, the tin halide addition is the most efficient and fabricates tin-based perovskite films. In 2016, Lee et al. introduced an innovative construction approach for $FASnI_3$ PSCs featuring a mesoporous n-i-p device structure. The resulting photovoltaic cells achieved a respectable PCE of 4.8 percent and exhibited excellent repeatability

pg. 58

[135]. Later, Liao et al. revealed a reversed p-i-n structure with a PCE of 6.22 percent [136]. Recent research has demonstrated further improvement of the PCEs up to 7-8%, which appears to be the best we can currently do using pure FASnI$_3$ perovskite [137, 138].

By partially replacing formamidinium (FA) with alternative organic cations, it is possible to achieve higher PCEs. For instance, Bian's and Huang's research teams achieved PCEs of 8-9% by substituting 25% of FA with methyl ammonium (MA). This substitution improved film shape and reduced carrier recombination [139]. Likewise, the attainment of PCEs exceeding 9 % was observed when a hybrid perovskite film was formed by incorporating a voluminous organic compound such as phenyl ethyl ammonium (PEA$^+$) into the FASnI$_3$ perovskite structure [140]. Diau's group has recently showcased a technique to produce superior perovskite film by combining guanidium (GA$^+$)/FA mixed cations and ethylene diammonium diiodide (EDAI$_2$) as an additive. This resulted in a remarkable 9.6 percent power conversion efficiency (PCE), surpassing the previously reported highest efficiency for tin-based PSCs [141]. Recent studies found that a mixed perovskite film of FA/DEA, which underwent post-treatment to analyze the Lewis base, achieved a PCE of 10.18 percent [142].

Table 3: Photovoltaic characteristics of ASnX$_3$ PSCs made with various deoxidizers

Deoxidizer	Configuration	J$_{SC}$ [mA cm^{-2}]	VOC [V]	FF [%]	PCE [%]	SPCE [%]	References
HPA	FTO/TiO$_2$/Al$_2$O$_3$/CsSnIBr$_2$/Spiro/Au	17.40	0.31	57.00	3.20	-	[143]
KHQSA	ITO/NiOx/FASnI$_3$/PCBM/Ag	17.64	0.552	69.40	6.70	5.73	[144]
Hydrazine vapor	FTO/TiO$_2$/CsSnI$_3$/PTAA/Au	30.75	0.17	34.88	1.83		[132]
	FTO/TiO$_2$/CsSnBr$_3$/PTAA/Au	13.96	0.366	59.36	3.04	-	[132]
	FTO/TiO$_2$/MASnI$_3$/PTAA/Au	19.92	0.377	51.73	3.89		[132]
N$_2$H$_5$Cl	ITO/PEDOT: PSS/FASnI$_3$/PCBM/BCP/Ag	17.64	0.455	67.00	5.40	4.72	[145]
THDH	ITO/PEDOT: PSS/FASnI$_3$/PCBM/BCP/Ag	22.12	0.54	50.00	8.48	7.47	[146]
Tin powder	ITO/PEDOT: PSS/FASnI$_3$/C60/BCP/Ag	17.50	0.58	66.30	6.75	5.70	[147]

3.1.2: Comparison of Lead and Tin-based PSCs

The slower progress in the performance of tin-based PSCs compared to lead-based PSCs can be attributed to two main challenges: the low chemical stability of divalent tin ($Sn2^+$) within the perovskite structure and the challenges associated with controlling the film morphology of tin-based perovskites [129, 148]. Despite the improvements in film quality, such as coverage, grain size, and crystallinity, observed in the mixed-cation perovskite films mentioned earlier, the vulnerability of $Sn2^+$ persists in these perovskites. To enhance the performance of devices and improve the stability of tin-based perovskite films, it is possible to introduce an antioxidant protective layer produced in-situ [144, 149].

To enhance the effectiveness of perovskite solar cells utilizing SnO_2, efforts are being made to increase their efficiency, Du et al. [150], in low temperatures, a layer composed of an amino acid or a self-assembled glycine layer is applied onto the SnO_2-ETL to serve as a buffer. This buffer layer adjusts the lattice mismatch between the perovskite layer and SnO_2 while enhancing the interaction between SnO_2 and the perovskite through electrostatic interactions between the amino group and the perovskite framework. Figure 6 provides a visual representation of the device structure of the perovskite solar cell based on SnO_2, as depicted in a schematic illustration [150]. This reduces the recombination of charge carriers and enhances the efficiency of charge carrier transportation. The researchers reported that the glycine-modified SnO_2-based perovskite solar cell achieved an impressive efficiency of 20.68 percent, with J_{sc} of 24.15 mA/cm^{-2}, Voc of 1.10 V, and FF of 0.78. The combination of SnO_2/glycine can act as an exceptional electron cushion sheet in extremely competent PSCs, as demonstrated by enhanced productivity.

Furthermore, triplex metallic oxides have greater features than dual metal oxides. In ternary metal oxide materials, it is possible to determine the relative proportions of the cations changed. As a result, optoelectronic characteristics like bandgap and electric resistivity can also be controlled. As a result, $BaSnO_3$ is an example of ternary metal oxides [151], $SrTiO_3$ [152], Zn_2SnO_4 (ZSO) [153], etc., ZSO stands out among ternary metal oxides as a favorable option for perovskite solar cell development due to its exceptional qualities. It possesses numerous advantages, such as a wide optical bandgap of 3.8 eV, high electron mobility ranging from 10 to 30 $cm^2V^{-1}s^{-1}$, and a suitable conduction band edge. These remarkable features make ZSO an appealing material for electrode selection in the quest for highly efficient perovskite solar cells [153]. This marks the initial occurrence of Oh et al. [154] conveyed a PCE of 7% for the ZSO ETL-based perovskite photovoltaic compartments. Later, Shin et al. [155] revealed an innovative method for generating ZSO nanoparticles for photovoltaics. The formed ZSO nanoparticles used to make the perovskite solar cells have 15.3 percent of PCE. Subsequently, Jung et al. [156] employed the film of ZSO processed through a solution that serves as an electron transport layer (ETL) in the world record-setting 20.02 % perovskite solar cell. Recently, a straightforward, affordable method called hydrothermal synthesis by Zheng et al. [157] single Zn_2SnO_4 crystal was made synthetically. The proposed method enables control over the dimensions of units and the shape of the ZSO solitary quartz through the hydrothermal reaction period.

Furthermore, utilizing ZSO single crystal in perovskite solar cells demonstrates an impressive PCE of 18.32% and a significant short-circuit current (JSC) of 24.79 mAcm^{-2}. Moreover, even after being subjected to 20% humidity for 15 days, the device maintains its stability. Considering these outcomes, it is evident that ZSO holds excessive potential as an ETL contender for producing remarkably effective photovoltaic strategies.
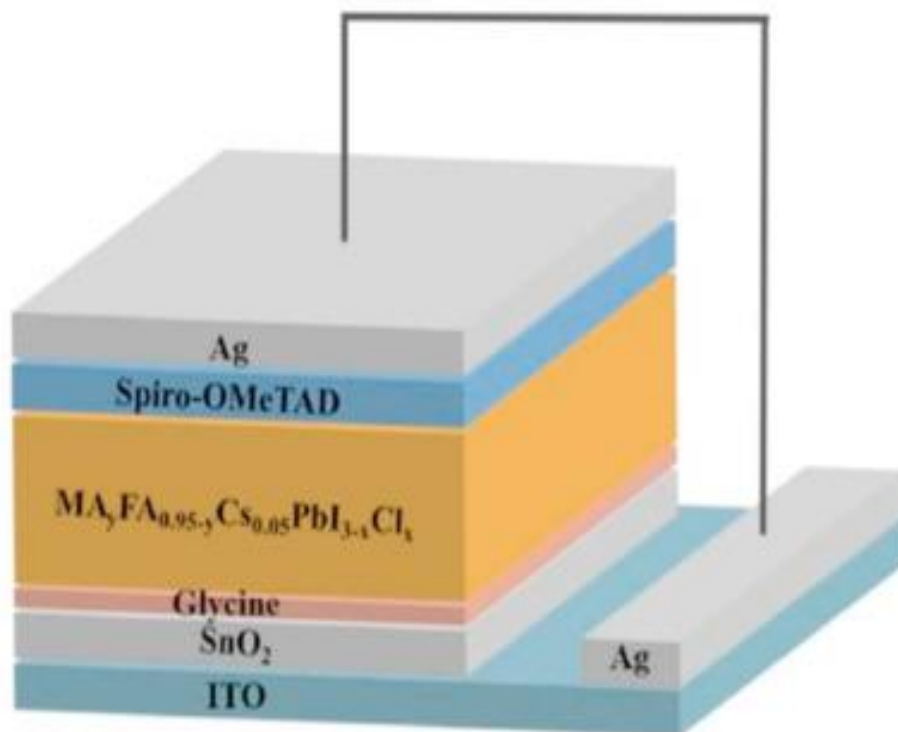
Figure 6: A schematic representation is provided for perovskite solar cells that utilize SnO$_2$ as their foundation [150].

3.2: Non-metal-based PSCs

Perovskite solar cells face commercialization challenges due to the high cost of organic HTL components and noble metals, despite being crucial elements in modern perovskite photovoltaic structures [158]. Despite being essential elements in contemporary perovskite photovoltaic systems, the high cost of organic HTL components and noble metals presents commercialization challenges for perovskite solar cells [159]. The HTM-unrestricted carbon-based-perovskite photovoltaic compartments have garnered significant consideration recently and achieved a record-breaking PCE of 16.37 %. These C-PSCs exhibit exceptional resistance to moisture and can be manufactured at a minimal cost [160]. Although C-PSCs offer advantages, they suffer from various limitations, with their relatively low PCE being a prominent drawback compared to conventional perovskite solar cells.

Additionally, in C-PSCs, the interface between the ETL and the perovskite is the sole interface that efficiently segregates the electron-hole pair. This ETL, which connects the electrode to the perovskite captivation film, facilitates the extraction of photo-generated electrons from the absorption layer and guides them toward the electrode. Consequently, choosing ETL material becomes crucial as it significantly enhances performance and constancy in C-PSCs. Moreover, the ETL acts as a barrier against holes, effectively inhibiting the recombination of electron-hole couples [161]. Recent investigators are fascinated by producing advanced ETL constituents that are optimized in this favour. Due to its exceptional optoelectronic properties, lack of toxicity, and strong chemical stability, TiO$_2$ is broadly employed as an ETL in PSCs [162]. The movement of charge carriers generated by light in perovskite solar compartments occurs through the perovskite and ETL interface. In the context of HTL-free C-PSCs, there is a problem of leakage of photocurrent caused by the acquaintance of the perovskite sheet by the ETL. This leakage negatively disturbs the routine of the manoeuvre. To address this issue and enhance

pg. 61

the device's effectiveness, a solution is to introduce an insulating layer composed of SiO_2 and ZrO_2 among the perovskite and ETLs [163].

Furthermore, the enhancement of TiO_2-based carbon perovskite solar cells (C-PSCs) performance can be achieved by incorporating methyl ammonium (MA) amino groups. However, deceptions, oxygen situations on the surface, and the interaction between TiO_2 and amino assemblies contribute to a decrease in C-PSCs' PCE [67, 164]. The latest findings indicate a significant enhancement in C-PSCs' PCE by incorporating a ferroelectric oxide ($PbTiO_3$) layer between the perovskite and TiO_2 [165]. Enhancing the electron transport competence further, Tao et al. [166] a $TiO_2@PbTiO_3$ core-shell structure was synthesized through an in-situ reaction to create mesoporous ETL material, which was subsequently utilized in C-PSCs. The researchers observed a significant reduction in defect density on the TiO_2 surface and decreased interfacial charge recombination due to the presence of the $PbTiO_3$ coating. The resulting C-PSC manoeuvre constructed using $TiO_2@PbTiO_3$ ETL displayed a favourable power conversion efficiency (PCE) attributed to the diminished Trap states. Based on their findings, the $TiO_2@PbTiO_3$ ETL-based C-PSCs exhibited an amended PCE of 7.97%, surpassing the PCE of $PbTiO_3$-free C-PSCs which achieved 6.55%.

3.2.1: Preparation method

Further, Du et al. [167] described a refined two-step sequential deposition method designed explicitly for synthesizing methyl ammonium lead bromide ($MAPbBr_3$) suitable for carbon-based perovskite photovoltaic cubicles. The researchers employed this approach to produce $MAPbBr_3$ perovskite films with minimized exceptional thickness, enhanced crystallinity, and extended transporter lifetime. The initial step involved introducing small quantities of MABr into the precursor solution of $PbBr_2$. Their study highlighted the utilization of these perovskite films for creating HTL-free C-PSCs. Under optimized conditions, the perovskite solar cells achieve an impressive PCE of 7.64 percent. The carbon-based $MAPbBr_3$ PSCs developed in this study maintain 95% of their initial PCE after being stored for 120 hours at 353 K, with relative humidity ranging from 40% to 70%.

Moreover, the manufactured carbon-based solar cells exhibit remarkable thermal stability, remaining highly stable when exposed to dry air and kept at room temperature. Notably, the PCE of these carbon-based solar cells remains unchanged for over a year, showcasing their long-term stability. As a result, this novel two-step sequential deposition method presents a promising approach to producing durable perovskite solar cells using carbon materials.

3.2.2: Non-metal based Structural Properties

A possible light source is also inorganic $CsPbBr_3$ quantum dots, which have good luminescent characteristics. Zeng et al. [168], in numerous reports, it has been stated that inorganic $CsPbBr_3$ perovskite-based LEDs exhibited an exterior dramatic productivity of 0.12 percent and a luminescence intensity of 946 $cdcm^{-2}$. Various studies have investigated the luminous characteristics of these LEDs [169, 170]. Moreover, the perovskite composed of $CsPbBr_3$ showcases remarkable endurance in low cell efficiency situations thanks to its optical band gap measuring 2.3 V. $CsPbBr_3$-based perovskites hold great potential in the development of innovative carbon-based inorganic perovskite solar cells due to their ability to maintain stability under ambient conditions, having a well-balanced band gap, and being prepared easily using the dual-source evaporation method, Ma et al. [171] researchers have demonstrated perovskite solar cells based on carbon-based $CsPbIBr_2$, displaying an impressive PCE of 4.7%. Next, Zhu et al. [172] an article detailed the features of perovskite solar cells composed of carbon-based $CsPbIBr_2$,

produced using a precursor solution of CsPbIBr$_2$. These C-PSCs achieved a peak PCE of 5.7%. Notably, the one-step spin coating technique was employed in their fabrication, Wang et al. [173] by meticulously regulating the temperatures of the substrate during preheating and post-annealing stages, a superior film of CsPbIBr$_2$ Perovskite with excellent quality was successfully produced. They claimed that the optimum temperatures significantly improved the produced perovskite films' crystallinity and light-absorbing capabilities, lowering charge carrier recombination. As a result, the proposed multistep solution spin coating method showcases an innovative approach to generating perovskite films of exceptional quality.
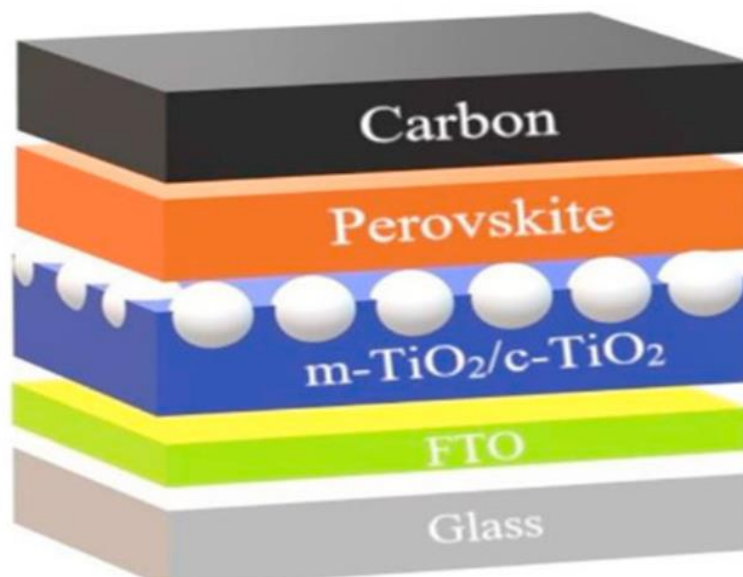
Figure 7: The image depicts a perovskite solar cell device PSC utilizing carbon-based CsPbBr$_3$ [174].

Enhancing the local connections between HTM/Perovskite and HTM/back-electrode interfaces leads to improved extraction of photo-generated charges in the presence of carbon materials and HTMs. This, in turn, significantly enhances the performance of the photovoltaic device [175]. In this framework, Zong et al. [176], using inorganic-organic molybdate/polyaniline-pyrrole hybrids, have been demonstrated to generate MoO$_2$/N-doped carbon nanospheres.

MoO$_2$ dispersion results from the uniform distribution of liquid phase precursors within MoO$_2$/N-doped carbon nanospheres. Furthermore, introducing nitrogen (N) doping enhances the conductivity of the nanospheres and reinforces the connection between the HTM and the perovskite surface [177]. They asserted that the utilization of MoO$_2$/N-doped carbon nanospheres prepared in their original state as the HTM in perovskite photovoltaic cubicles resulted in a reduction of surface imperfections and boosted holes abstraction at the boundary among perovskite and carbon. Consequently, the CsPbBr$_3$ PSCs incorporating MoO$_2$/N-fixed carbon nanospheres demonstrated improved PCE. Zong et al. [176] constructed CsPbBr$_3$ perovskite photovoltaic compartments with a maximum PCE of 9.4% consuming the generated nanospheres as HTMs.

Additionally, the paired device displays a PCE of 6.86 percent without HTM, and the device with HTM exhibits significantly lower values than its counterpart. Further, the manufactured solar cell demonstrates exceptional stability, lasting more than 800 hours at 80 percent comparative moisture. These findings indicate that C-PSCs incorporating inert HTMs outperform those lacking HTMs. Graphene, a semiconductor with a zero-band gap and semi-metallic properties, exhibits electrical characteristics

determined by the π-π bonds connecting its carbon atoms. The conductivity of graphene is governed by the out-of-plane π-bond, from which the delocalized electrons originate. These electrons exhibit a carrier mobility of up to 2 x 105 cm^2 V^{-1} s^{-1} when moving. The remarkably low state concentration of the Dirac point enables the alteration of graphene's work function through carrier injection. Graphene's work function and conductivity type can be effectively modified by introducing metallic and non-metallic atoms and molecules.

Numerous treatment methods have been created to use graphene derivatives in solar cells. Table 3 enumerates various adjustments made to the work function of graphene to suit its applicability in solar cell manufacturing. These adjustments involve multiple processes, such as exfoliated graphene oxide (GO) and its condensed form (rGO), with the degree of reduction or oxidation serving as a means to manipulate the conductivity of graphene [178].

Table 4: Optimization of the graphene exertion purpose through SC application tuning

Material	Work function	Treatment	Role	SC type	PCE, %	References
GO	4	Cs_2CO_3	ETL, an active layer	organic	3.67	[179]
rGO	4.3	1-pyrene carboxylic acid grafting	ETL, an active layer	organic	2.85	[180]
GO	4.3	Li_2CO_3	ETL	perovskite	11.14	[181]
GO	4.68	silver trifluoromethanesulfonate	HTL	perovskite	11.9	[182]
GO	4.8	fuming sulfuric acid	HTL	organic	4.37	[183]
CVD graphene	4.8-4.95	$AuCl_3$	HTL	perovskite	15.9	[184]
rGO	4.84-4.88	p-toluene sulfonyl hydrazide	HTL	organic	3.63	[185]
GO	4.89-4.99	$OsCl_3$, $PtCl_4$, and $AuCl_3$	HTL	organic	3.54	[186]
rGO	4.95	Ag - microwave-assisted	An Active layer, hole extraction	organic	4.23	[187]
rGO	4.97	Phenyl hydrazine-based reduction	HTL	organic	6.71	[188]
GO	5.2	O_2 plasma treatment	HTL	organic	3.59	[189]
GO	5.21	photochemical chlorination	HTL	organic	7.59	[190]
GO	5.23	photochemical chlorination	HTL	organic	6.56	[191]
GO	5.37	NH_3	HTL	perovskite	16.11	[192]

3.2.3: Application

Continuing with this, Yang et al. [193] recommended a modest technique for manufacturing carbon rods for C-PSCs. An unrestricted-vertical carbon deposit is hot compelled onto the HTL of perovskite solar cells in the recommended method. The conductivity of the electrode was boosted more than ten times due to the mono-flexibility of the carbon sheets produced. Additionally, the hot-persistent technique enhanced the bordering film of the carbon electrode. They described that improvements in multiple mechanical and electrical properties occur at an optimal applied temperature of 80 C, significantly improving device performance. Moreover, the PSC with a hot-compelled carbon probe demonstrates a PCE of 15.3 percent, which is 70 percent more than the PCE achieved by the standard temperature device. Furthermore, the PSC with the carbon electrode maintains 93% of its original PCE even after 80 days of operation under relative humidity ranging from 55% to 70% without encapsulation. These aspects indicate that the simple procedure offers a fresh approach to generating exceptionally efficient perovskite solar cells for the next generation.

3.3: CARBON MATERIALS IN SINGLE-JUNCTION PSCs

Given the affordability, hydrophobic properties, remarkable transparency, conductivity, elasticity, and other notable attributes, different natural resources emerge as up-and-coming options for utilization in PSCs. Carbon-based materials like fullerene, carbon black, graphite, CNTs, graphene, and others have been employed in PSCs. This segment will examine current advancements related to carbon constituents' electrodes, charge transportation, and perovskite deposits. This discussion will focus on PSC module application research, considering the extensive available research in this area [194].

3.3.1: Electrodes composed of carbon

Due to several factors, Carbon has gained significant usage as a different conductor substantial to metallic cathodes in perovskite solar cells. Firstly, the various allotropes and exceptional properties of carbon materials have the potential to improve PSC performance significantly. Secondly, employing a flexible and hydrophobic carbon film as a protective layer is highly effective in enhancing the stability of PSCs. Lastly, carbon stands out as a preferred material for PSCs due to its affordability and environmentally friendly nature [194].

3.3.2: Stability improvement

The cell only lasted for around ten minutes in the early phases of PSC formation (80 % degradation) [195]. Stability remains a crucial concern in the ongoing development of future PSCs. Enhancing the hydrophobicity of carbon materials to ensure functional stability and optimizing their flexibility for mechanical stability can potentially extend the service life of PSCs significantly. The hydrophobic qualities of carbon compounds help minimize moisture-related deterioration and enhance strength in PSCs [196]. Siram et al. [197] investigated the permanency of PSCs using regular Au electrodes and MWCNTs modified with organic nanocrystals under four distinct conditions. After approximately 45 days of stability testing at 25°C and 25 to 35 percent comparative moisture, the power conversion efficiency (PCE) of encapsulated perovskite solar compartments with Au significantly declined. However, the PCE of cubicles incorporating MWCNTs remained remarkably steady subsequently 60 days of challenging. MWCNT-based PSCs were also more resilient during photo stability testing in natural lighting conditions. Then again, Raminafshar et al. [198] proved the carbon electrode's ability to withstand moisture. All of their PSC cells had a PCE of about 10%. Over four months, while maintaining an ambient temperature of

approximately 25° Celsius and humidity level ranging from 20% to 30%. To enhance the firmness of perovskite solar compartments, the hydrophobic carbon layer efficiently prevented humidity from penetrating the PSC. Furthermore, flexible PSCs' mechanical strength was also credited to the flexibility of films made of carbon. Yoon et al. [199] produced a PSC with a highly bendable graphene electrode. PCE was 16.8% in a 1.77 mm^2 device without hysteresis. Following 1000 rounds of bending with a radius of 2mm, the flexible device maintained 90% efficiency, while the PCE of compartments invented on conformist indium tin oxide (ITO)/polyethene naphthalate (PEN) substrata was lower. However, subsequently 1000 winding sequences with an area of 4mm, the PCE dropped to 40%. Jang et al. [200] created a new flexible PSC, resulting in a forward PCE of 10.96% and a reversed PCE of 11.16%. The PSC employed a graphene electrode with modifications and silver (Ag) reflectors on both cell sides. The PCE remained consistent after undergoing 1000 bending cycles with an 8-mm radius, retaining over 70% of its initial value.

3.3.3: Performance improvement

The tuning of specific characteristics of carbon ingredients, such as exterior irregularity, viscosity, and hole extent, enables the enhancement of interfacial interaction between the carbon rod and the primary film. A tiny, porous carbon self-adhesive sheet created by Zhang et al. [201] was made using a low-temperature solvent conversation method that prevented the carbon residue from hardening. The weaker curative, considered one of the primary causes of roughness, prevented the development of carbon blocks and bulges. Following 80 hours, the PSC PCE of the sample reached 19.2 percent while retaining over 94 percent of its primary proficiency. A cell produced through a predictable method needing a high strengthening temperature displayed a lower power conversion efficiency (PCE) [202] of just 15.2 percent. In accumulation, Ryu et al. [203] devised a new method to link the perovskite layer and carbon electrode by utilizing multi-walled carbon nanotubes (MWCNTs) as connectors, employing a unique solvent-dripping technique. The hole transmission proficiency among two sheets might be improved primarily by the paths that the bridges formed. The leading device achieved a (PCE) power conversion efficiency of 13.57 % without hysteresis, whereas the average efficiency of cells modified with multi-walled carbon nanotubes (MWCNTs) was 11.5 percent. Despite carbon ingredients having less conductivity than gold (Au), extensive examine has been dedicated to reducing resistance by adjusting factors such as doping, crystallinity, or morphology. For example, graphite-constructed films exhibit comparatively higher conductivity related to graphene and solitary-partition carbon nanotubes. Enhancing the graphite conductivity films can be achieved by employing higher and further homogeneously sized graphite. Thus, one can enhance the conduction of the carbon electrode; Jiang et al. [204] a film of carbon adhesive was developed, which exhibits excellent conductivity and sheet resistance of 4Ω/sq. This achievement was accomplished by carefully selecting appropriate dimensions of black lead and regulating the carbon dusky to graphite ratio. According to their research, better graphite was produced by larger, more homogeneous graphite particles. Higher conductivity was achieved thanks to improved graphite particle interaction and fewer antiparticle spaces. Similarly, Zhang et al. [205] also found a correlation between the size of the graphite and the conductivity of graphite Film. Additionally, P-type doping can significantly reduce the carbon film's sheet resistance. Chu et al. [206] utilized carbon electrodes doped with p-type NiO nanoparticles to lower the charge transfer resistance. The doped cell's PCE was 13.26 percent.

3.3.4: Economic benefits

Additionally, carbon-based electrodes benefit from being inexpensive and having a straightforward manufacturing process. Meng et al. [207], a specific hot-press technique, was employed to develop an affordable and dependable coal-based perovskite photovoltaic compartments, achieving 10.87 percent of

PCE (0.3 cm^2) and 8.72 percent (1 cm^2). Wei et al. [208] established a novel link between potassium and carbon dioxide, converting CO_2, a greenhouse gas, into a honeycomb-like graphene structure. This graphene-based film was utilized as an electrode in a high-throughput, low-temperature-free Perovskite Solar Cell (PSC) with a remarkable PCE of 10.06 percent.

3.4: Polymer-based PSCs

Lately, scientists have been attentive to enhancing the constancy of perovskite solar compartments through the implementation of device encapsulation [209], connectional adjustment [210], and a reversed arrangement [211], so forth. Conferring to information, essential modification can also rise the constancy of perovskite, mainly by dipping damp erosion [212]. Typically, the functional layer is focused on interfacial alteration [213]; ETL, HTL, photovoltaic, and buffering layers are examples. On the other hand, the intergranular interface, commonly referred to as the perovskite contact, exhibits a greater concentration of defects [214]; due to this, moisture can spread quickly into the perovskite film [215, 216]. Thus, increasing the crystallinity at the intergranular contact is essential, improving the perovskite film's shape, charge transfer, and separation [177]. An outstanding photovoltaic performance was produced due to the perovskite film's increased charge separation and transport. As a result, the moisture resistance of perovskite intergranular interfaces is enhanced, leading to improved stability in perovskite solar cells [216]. Scientists are dedicated to strengthening the interactions among perovskite grains, which involve various aspects such as p-p stacking, hydrogen attachment, acid-base reactions, electrostatic interactions, etc., to create an intergranular interface resistant to moisture [214]. For instance, substituting phenethylamine for methylamine (CH_3NH_2) might increase p-p assembling and hydrophobic interactions ($PhCH_2CH_2NH_2$). In addition, the hydrogen bonding relationship is enhanced when formamidine replaces methylamine (CH_3NH_2). Due to the abundance of active sites, perovskite solar cells exhibit superior quality in terms of their PCE and stability [217], polymers like polymethylmethacrylate are examples of (PMMA) [218], polyethylene oxide (PEO) [219], polyvinylpyrrolidone (PVP) [220], polyethyleneimine (PEI) [221], etc., demonstrate the firm contacts between granules. Strong intergranular interactions result in good stability and improved PCE in polymer-based photovoltaic devices [222]. All of the described polymers alter the curly macromolecular architecture of the perovskite to modify the intergranular interactions. Otherwise, they will have an adverse outcome, such as falling the perovskite's crystallinity or failing its photoelectric property, between other effects. Scientists are working to offer a novel group of polymers with an improved assembly in direction to solve these contests.

3.4.1: Polymer-based Structural properties

Dendrimers, also known as dendritic polymers, are regarded as having spherical shapes and receiving a lot of interest. Because molecular arrangement enables modest procedure adjustment when interacting with the surface of perovskite granule, it also avoids indigenous categorizing inside the distinct linear-macromolecular design [223]. The dendrimers' crystallinity is enhanced as a result. Consequently, polymers with dendritic structures can successfully increase the constancy and effectiveness of perovskite strategies. Enduring with this, Du et al. [224] twisted a unique biological protocol to irradiate the performance of perovskite photovoltaic compartments. The suggested model successfully controls perovskite intergranular contact, enhancing PCE. Du et al. [224] utilized dendrimers of polyamidoamine (PAMAM) as a dendritic to form a crystal structure to template perovskite's crystallization. The PAMAM comprises methyl phenyl acetates at the molecular perimeter, and its carbonyl & amino groups have a lot of interfacial ability in the perovskite's granule surfaces.

pg. 67

As a result, the perovskite granules developed strong intergranular interfacial contacts and were interlinked with a framework of dendritic polymer. Additionally, the perovskite phase's shape is significantly improved by eliminating the pinholes and dropping the grain margins. Therefore, the perovskite grain's dendritic PAMAM crosslinking increases the contacts at the intergranular perovskite interface and produces a homogeneous perovskite film with no pinholes and small size. As a result, at room temperature, the encapsulated perovskite photovoltaic compartments with the PAMAM dendritic-polymer framework had an elevated PCE of 42.6 percent. The PAMAM-modified gadget also exhibits 73% retention after 400 hours and retains its primary PCE. The primary feature in attaining huge PCE is the PAMAM modification, which enhances perovskite intergranular contacts. Figure 8 shows a schematic of how PAMAM dendrimers control the structure of perovskites and the design of a perovskite solar cell modified by PAMAM [224].

Additionally, interlayers are essential for increasing the perovskite photovoltaic compartments of PCE. Recently, Kang et al. [225] have demonstrated how the use of polyelectrolytes as buffer layers in both p-type (P-I-N) and n-type (N-I-P) substrates geometries affects the device's performance. To generate the buffer coatings, they used non-coupled NPEs having a poly (ethyleneimine) (PEI) support and an assortment of counter ions for example, bromide (B^-), iodide (I^-), and tetrakis (imidazole) borate (BIm^-_4). Additionally, the perovskite solar cell's performance varies depending on the size of the molecule.

At the NPE/metal electrode contact, non-coupled polymers generate electrical dipoles that can adjust the electrodes' work functions and energy levels. Geometries P-I-N and N-I-P, the PCE of the NPE buffer film-based photovoltaic device is 14.71 percent and 13.79 percent, respectively. The HTL layer typically extracts the shacks. It affects the efficiency of perovskite photovoltaic compartments preventing charge transporters from recombining at the perovskite-polymer interaction electrode. Therefore, developing the hole conveyance films is also required for creating perovskite solar cubicles that work well [226]. Due to its excellent film structure, more conductivity, and ease of solution processing Poly(ethylene dioxythiophene) (PEDOT): poly (styrene sulfonate) (PSS) at low temperatures has been one of the most widely utilized HTLs in perovskite reversed photovoltaic cubicles up to this point [227]. Despite the benefits, PEDOT's acidic nature: One of the significant PEDOT restrictions is PSS. HTL is based on perovskite photovoltaic compartments PSS [228]. Numerous scientists are searching for innovative concepts and approaches to enhance device efficiency by addressing the disadvantages of PEDOT: PSS HTLs [229, 230].
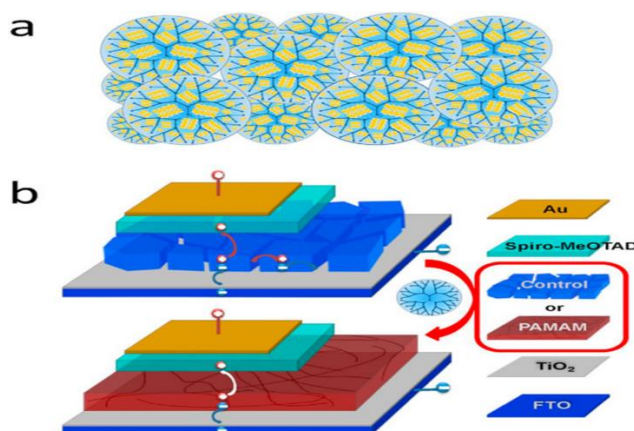
Figure 8: a) Diagrammatic illustration of PAMAM dendrimers controlling the structure of perovskite b) Device arrangement of regulator and PAMAM-adapted perovskite photovoltaic compartments [224].

3.4.2: Applications of Perovskite Solar Cells

PSCs have used various strategies to attain high performance, including switching from photovoltaic frameworks that have been sensitized to more modern photovoltaic compartments with planar thin sheets, making perovskite-light-active hybrid ingredients, utilizing manufacturing conditions, and, finally, using various charge ETMs and HTMs. Additionally, high-quality perovskite films are influenced by PSC production techniques. Recently, Xu et al. [231] offered a creative process using widely accessible copper (I) thiocyanate to create a new HTL (CuSCN). They claimed that adding CuSCN to PEDOT: PSS and, subsequently, low-temperature annealing enhanced charge extraction performance while lowering the energy barrier and neutralizing the acidic nature of the material. A 16 percent improvement over PSS-HTL-based perovskite photovoltaic compartments based on PEDOT can be seen in the PSS-HTL-based PCE of CuSCN-modified PEDOT perovskite photovoltaic framework, which is 15.3 percent at VOC of 1.0 V. Additionally, lower acidity produces exceptional long-lasting reliability; for example, 71% of the device's primary PCE is retained after 175 hours of interaction to N2 at a total capacity of solar light. Ma et al. [232] presented a tiny diphenylamine-created NPB as a multifunctional in a perovskite photovoltaic framework; a layer of buffer material is used to enhance PCE. NPB is an acronym that stands for N, N'-(Bis-(1-naphthalene)-N, N0 -bis-phenyl-(1, 10 -biphenyl) 4 or 40 -diamine. The structure of the NPB-based perovskite photovoltaic compartment is shown in figure 9 [232].

According to their findings, adding NPB to a perovskite film decreases flaws and pinholes and modifies the disparity in energy levels between the PEDOT: PSS film and the framework. Because of the reduced pinholes and imperfections at the perovskite junction and PEDOT: PSS section, charge carrier recombination is severely constrained in devices improved by NPB. As a result, the PCE of the NPB-modified perovskite photovoltaic compartment is 18.4%. The identical device displays 14.4% PCE with no distortion and good consistency under UV light. According to the suggested method, building extremely stable, effective, and adaptable next-generation perovskite solar cells may depend significantly on the NPB acting as a buffering layer. Nearly all revealed the availability of bendable perovskite photovoltaic cubicles, tiny surface parts distant. Because of the unavoidable decrease in film homogeneity, it is commonly understood that the PCE is compressed when the position of the devices is magnified on a huge rule. Therefore, the routine of the large-part flexible perovskite photovoltaic cells is directly affected by the thin film deposition method on a big scale. Thus, all the layers in stretchable perovskite photovoltaic compartments require developing large-area procedures. Alternative technologies should be introduced to reduce fabrication costs, hopefully encouraging actual applications' realization. Below are some available approaches [232].
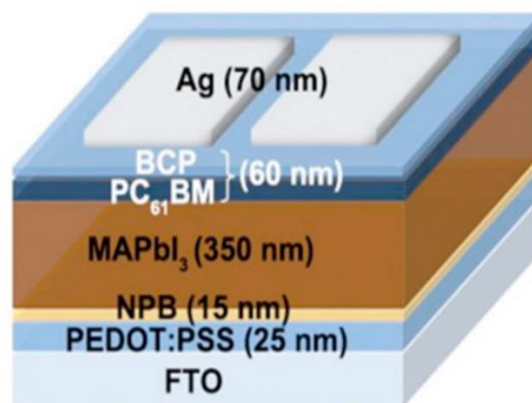
Figure 9: The structure of the NPB-based perovskite photovoltaic compartments device [232].

pg. 69

3.4.2.1: One-Step Method

As shown in figure 10a, the process of spinning covering a perovskite forerunner solution onto a translucent conductive oxide platform before sintering to form the perovskite energetic sheet is the single-step deposition process. The most popular deposition technique since it is straightforward and inexpensive to produce for tiny PSCs developed in a lab. Still, it is not appropriate for fabricating extreme surface-area devices. Dimethyl sulfoxide (DMSO), dimethyl form amide (DMF), or γ-butyrolactone (GBL) are examples of common dipolar aprotic solvents, which are used to dissolve organic (such as FAI/MAI/) and inert (for example, SnX_2/PbX_2/) halides to create a perovskite film with the quartz assembly ABX_3 that is then twist-layered onto a conductive substratum involving ETM. The initial PSC production that sparked the objective of the investigation was achieved by spinning natural salts (MABr and MAI) in a single step combined with inert salts ($PbBr_2$ or $PbCl_2$), with the resulting $MAPbBr_3$ and $MAPbI_3$ PSCs achieving efficiencies of 3.31 percent and 3.81%, respectively [42]. Miyasaka (2012) claimed efficiency levels of up to 10.9 % in a later investigation by spin covering a mesoporous Al_2O_3 scaffold with a mixed-halide perovskite precursor mixture [78].

The ionic strength of the fluid and post-annealing improves the properties of perovskite crystal production in the one-step deposition process [234]. However, issues including morphological control and a lack of film consistency are seen. Chen (2015) 210 nm-thick perovskite was used to create a perovskite instrument that is inverted (p-i-n) in a single step of spin coating, yielding PCE of 11.99%, J_{sc} of 21.9 $mAcm^{-2}$ and V_{oc} of 0.81 V.
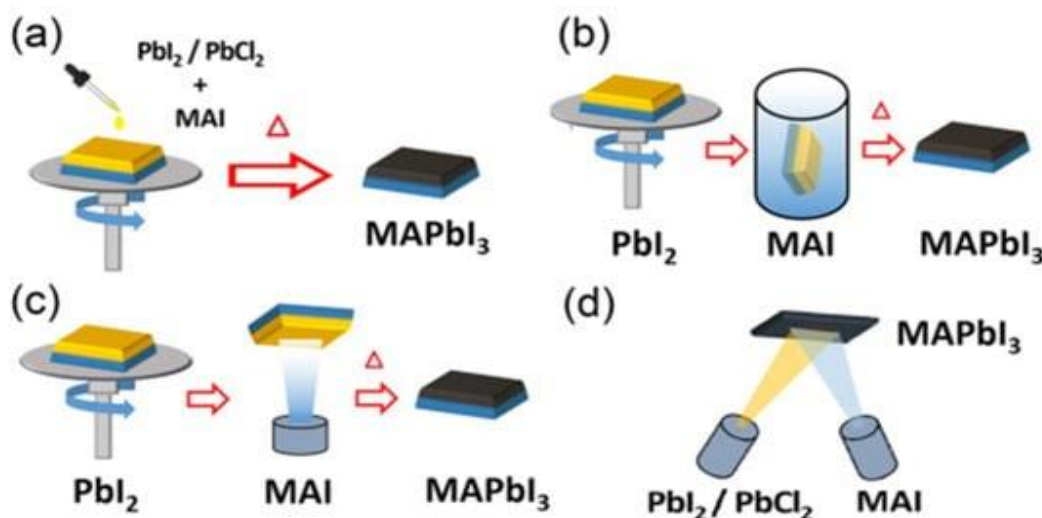
Figure 10: Methods for manufacturing perovskite solar cells are shown schematically. (a) One-phase procedure; (b) second stage process; (c) Method of Vapor-Sponsored result; (d) thermal vapour deposition technique. Amounts of precursors, wrapping reducing time, coating rotation time, and shifting speeds are fabrication-controlling factors for perovskite film quality or shape [233].

Zhang (2019), engineering techniques based on binary solvents improved the perovskite surface morphology during the one-step perovskite deposition. The process allows for comprehensive and well-organized homogenous perovskite sheets by controlling the production of perovskite crystals [236]. A

combination of solvents, including the DMF as mentioned above, DMSO, and GBL, is used to accomplish this particular control over the perovskite morphology [237]. Images of AFM can be found at various DMF/DMSO mediator ratios are one to one, three to one, and three to one, designated as FO_{10}, FO_{31}, and FO_{13}. The film helps in reducing the experimental morphological fissures, small holes, and an absence of crystallization flaws by adding another solvent in the ratios of 3:1 and 1:3. As a result, figure 16e shows the experimental significance, plane, and densely granular designs of stacked perovskite. Similar research was conducted using a 7:3 solvent mixture of GBL and DMSO; Jeon (2014) attained 16.2% efficiency in I-V evaluations of both forward and reverse bias without any hysteresis. [237].

3.4.2.2: Two-Step Method

Specific biological (MAI/FAI) and inert (PbX_2/SnX_2) antecedent solutions are spin-coated as part of the two-step manufacturing, also known as sequential fabrication. This approach can enable exterior morphology and film worth control by maximizing dip-varnishing or twist-varnishing times, precursor concentrations, and spinning velocities during carbon-based or inert halide precursor deposition. In the second stage process, PbX_2 is an inert halide that is spin-coated on a substratum as the first phase of the deposit; the organic MAI solution is then applied as the second coating phase involves either (i) depositing the PbX_2-coated substratum into the natural MAI resolution or (ii) rotation depositing it over the PbX_2 [238]. Using the two-step technique, Burschka (2013) created a PSC with a PCE of 15.0 percent. The study confirms that SEM cross-sectional micrographs and XRD examination of the device provide better control of the device's shape [239]. First, the PbI_2 injection into the nano-porous TiO_2 coating is visible in the presented cross-sectional SEM pictures. This has been demonstrated by successfully depositing PbI_2 into TiO_2 nano-pores by producing a single TiO_2/PbI_2 film with complete PbI_2 crystal fascination. The creation layer of perovskite absorber following another stage MAI deposition through (i) dip coating a PbI_2 /TiO_2 containing substrate is confirmed by the XRD design, which displays a distinctive at 14° diffraction angles, there is a perovskite peak.

PbI_2 residuals decrease the solar cell's capacity to capture light and move charge carriers, which lowers the PSC's overall performance [240]. Like the single-phase deposition approach described above, solvent engineering and extracts may be used to get around the binary-stage techniques manufacturing flaw. Li (2015) reported using a DMF and DMSO-based solvent mixture to dissolve PbI_2 powder. The solvent mixture's DMSO works as an intermediary exchange agent with MAI during the creation of the $MAPbI_3$ film, delaying the onset of PbI_2 crystallization. Perovskite crystals only develop at the PbI_2 surface due to little heat and brief varnish time of MAI through another deposition phase, preventing additional MAI permeation into the PbI_2 framework. A rough surface structure with spaces and pinholes is created by mass infiltration [241].

3.4.2.3: Method of Vapor-Sponsored Solution

The vapour-assisted solution ejection technique modifies the two-step approach, which enhances the precursor solutions' penetration. The two-phase method and the solution aided by vapour differ only in the second depositing process, which involves reacting a vapor stage with the PbI_2 sheet of either MAI or FAI [242]. Chen (2015) found the effectiveness of PSCs made using the vapour-assisted and binary-phase solution techniques was examined, and it was found that distinct fabrication methods produce PSCs with varying attributes of flat films using vapour-assisted deposition exhibit high mesoporous TiO_2 covering of the surface and pour filling. The device's concert over the 400–740 nm wavelength range shows the highest Voc of 0.96 V with an IPCE score of 81 %. The two-step manufactured film's Spectra of photoluminescence (PL) revealed an extreme epitome, which confirmed defect concentrations brought on

by inadequate surface covering [243]. This study demonstrates that the vapour-assisted solution method has higher device efficiencies than the two-step procedure. The time-consuming deposition of MAI vapour is a drawback of the vapour-assisted approach [244].

3.4.2.4: Thermal Vapor Deposition Method

In the heat-transfer vapour expulsion approach, organic (such as FAI or MAI) and manufactured (such as $PbCl_2/PbI_2$) halides are simultaneously deposited on a spinning substrate in the vapors phase. As a result of the simplicity of controlling the parameters for precursor deposition and the rotational speed of the substrate, this approach provides a homogeneous surface morphology [245]. Liu (2013) revealed a 15.4% increase in planar mixed-halide PSC recording efficiency. The $MAPbI_3$-xClx perovskite thin films were created using the 4:1 vapour deposition of precursor powder materials for MAI and $PbCl_2$ [43]. To create a PSC device with a vast surface area, Liang (2018) described a massive PSC with a 100 cm^2 surface area [246].

4: Development in perovskite photovoltaic cells

Perovskites made of organ lead halide have been utilized for solar chambers since 2009. Perovskite light absorbers were initially employed as sensitizers in liquid dye-sensitized solar sections. Because of its solid ionic nature, perovskite can be dissolved in polar strippers, which restricts the further progress of solar cells using perovskite-sensitized photo electrochemical technology. In 2012, a reliable fixed perovskite solar cell was created by swapping liquid for strong HTM. Perovskite solar cells are now referred to as solid-condition perovskite-containing photovoltaic cells. The Korean Investigative Association of Natural Technology houses the National Renewable Energy Laboratory (NREL) accredited, attained a 17.9 % PCE as of June 10th, 2014 (NREL) [247].

5: Future Research

This study comprehensively analyzed PSCs, promising photovoltaic (PV) technology that offers clean, affordable, and sustainable electricity for the future should be the main topic of future study. The forthcoming effort will focus on enhancing and innovating new approaches to enhance the performance of PSCs. To improve the extraction of electrons in PSCs use advanced materials, to increase the constancy of perovskite solar cells, converging on moisture and thermal conflict. Discover accessible developing skills such as roll-to-roll lithography to decrease expenses and improve manufacturing efficiency. Researchers will enhance the solidity and productivity of Perovskite films when using other traditional resources like silicon. Further improvement and increase in the elasticity and light captivation Properties of Perovskite researchers also used organic materials and anti-reflective coatings rapidly contributed to developing this innovative photovoltaic expertise. Attention on improving charge transport layer and edges to diminish energy fatalities and increase whole-cell proficiency. To reduce pollution, researchers also worked on lead-free materials, which are also beneficial for our environment and do not have bad effects on human health. In future researchers will also use advanced characterization methods such as synchrotron and electron microscopy for comprehensive exploration and arrangement of perovskite cells. Scientists use computational modelling for the development of new models of PSCs with the help of changing the conditions and strategy of architecture. Examine the perspective of market demand PSCs expertise on worldwide renewable energy adoption.

6: Conclusion

In summary, PSCs characterize an important development in photovoltaic expertise, offering huge proficiency, low manufacturing expenses, and very flexible application. The efficiency and constancy of perovskite solar cells have been improved by methods such as; generating electron and hole transport layers, expanding interfacial films, and considering tandem solar cells. In detail, investigation has been completed on tin-based, lead-based, and carbon-based perovskite solar cells, each of which has advantages and drawbacks. The examination of carbon and tin-based substitutes has resulted from exertions to decrease or eliminate lead absorption in PSCs. To sponsor the commercialization and extensive receiving of PSCs in industrial uses, further study should focus on improving the cost-effectiveness, constancy and scalability and making lead-permitted perovskite ingredients and advanced ETLs. Perovskite solar cells can modify or vary the clean energy countryside and contribute to a defensible and environmentally friendly upcoming with remaining perfections in scalability, solidity, cheapest and lead-free alternatives.

References

1. Mahmud, M.A., et al., Origin of efficiency and stability enhancement in high performing mixed dimensional 2D-3D perovskite solar cells: a review. Advanced Functional Materials, 2022. 32(3): p. 2009164.

2. Snaith, H.J., Perovskites: the emergence of a new era for low-cost, high-efficiency solar cells. The journal of physical chemistry letters, 2013. 4(21): p. 3623-3630.

3. Wong, A.B., et al., Growth and anion exchange conversion of CH3NH3PbX3 nanorod arrays for light-emitting diodes. Nano letters, 2015. 15(8): p. 5519-5524.

4. Senanayak, S.P., et al., Understanding charge transport in lead iodide perovskite thin-film field-effect transistors. Science advances, 2017. 3(1): p. e1601935.

5. Ji, L., et al., High-performance photodetectors based on solution-processed epitaxial grown hybrid halide perovskites. Nano Letters, 2018. 18(2): p. 994-1000.

6. De Wolf, S., et al., Organometallic halide perovskites: sharp optical absorption edge and its relation to photovoltaic performance. The journal of physical chemistry letters, 2014. 5(6): p. 1035-1039.

7. Wehrenfennig, C., et al., High charge carrier mobilities and lifetimes in organolead trihalide perovskites. Advanced materials, 2014. 26(10): p. 1584-1589.

8. Stranks, S.D., et al., Electron-hole diffusion lengths exceeding 1 micrometer in an organometal trihalide perovskite absorber. Science, 2013. 342(6156): p. 341-344.

9. Miyata, A., et al., Direct measurement of the exciton binding energy and effective masses for charge carriers in organic–inorganic tri-halide perovskites. Nature Physics, 2015. 11(7): p. 582-587.

10. Zhao, Y. and K. Zhu, Organic–inorganic hybrid lead halide perovskites for optoelectronic and electronic applications. Chemical Society Reviews, 2016. 45(3): p. 655-689.

11. Kumar, N.S. and K.C.B. Naidu, A review on perovskite solar cells (PSCs), materials and applications. Journal of Materiomics, 2021. 7(5): p. 940-956.

12. Ionescu, C., et al., The historical evolution of the energy efficient buildings. Renewable and Sustainable Energy Reviews, 2015. 49: p. 243-253.

13. Shukla, R., et al., Recent advances in the solar water heating systems: A review. Renewable and Sustainable Energy Reviews, 2013. 19: p. 173-190.

14. Karkas, M.D., et al., Artificial photosynthesis: molecular systems for catalytic water oxidation. Chemical reviews, 2014. 114(24): p. 11863-12001.

15. Hedley, G.J., A. Ruseckas, and I.D. Samuel, Light harvesting for organic photovoltaics. Chemical Reviews, 2017. 117(2): p. 796-837.

16. Sharma, S., K.K. Jain, and A. Sharma, Solar cells: in research and applications—a review. Materials Sciences and Applications, 2015. 6(12): p. 1145.

17. Battaglia, C., A. Cuevas, and S. De Wolf, High-efficiency crystalline silicon solar cells: status and perspectives. Energy & Environmental Science, 2016. 9(5): p. 1552-1576.

18. Feurer, T., et al., Progress in thin film CIGS photovoltaics–Research and development, manufacturing, and applications. Progress in Photovoltaics: Research and Applications, 2017. 25(7): p. 645-667.

19. Başol, B.M. and B. McCandless, Brief review of cadmium telluride-based photovoltaic technologies. Journal of photonics for Energy, 2014. 4(1): p. 040996-040996.

20. Carey, G.H., et al., Colloidal quantum dot solar cells. Chemical reviews, 2015. 115(23): p. 12732-12763.

21. Saparov, B. and D.B. Mitzi, Organic–inorganic perovskites: structural versatility for functional materials design. Chemical reviews, 2016. 116(7): p. 4558-4596.

22. Novoselov, K.S., et al., Electric field effect in atomically thin carbon films. science, 2004. 306(5696): p. 666-669.

23. Da Silva, D., et al., Application of amorphous carbon based materials as antireflective coatings on crystalline silicon solar cells. Journal of Applied Physics, 2011. 110(4): p. 043510.

24. Matsumoto, H., et al., Screen-printed CdS/CdTe solar cell of 12.8% efficiency for an active area of 0.78 cm2. Solar cells, 1984. 11(4): p. 367-373.

25. Kibria, M.T., et al. A Review: Comparative studies on different generation solar cells technology. in Proc. of 5th International Conference on Environmental Aspects of Bangladesh. 2014.

26. Yan, J. and B.R. Saunders, Third-generation solar cells: a review and comparison of polymer: fullerene, hybrid polymer and perovskite solar cells. Rsc Advances, 2014. 4(82): p. 43286-43314.

27. Wei, H. and J. Huang, Halide lead perovskites for ionizing radiation detection. Nature communications, 2019. 10(1): p. 1066.

28. Sun, S., T. Buonassisi, and J. Correa-Baena, Advanced Materials Interfaces. 0.

29. Yang, Y. and J. You, Make perovskite solar cells stable. Nature, 2017. 544(7649): p. 155-156.

30. Shi, Z., et al., Lead-free organic–inorganic hybrid perovskites for photovoltaic applications: recent advances and perspectives. Advanced Materials, 2017. 29(16): p. 1605005.

31. Abate, A., Perovskite solar cells go lead free. Joule, 2017. 1(4): p. 659-664.

32. Bagher, A.M., M.M.A. Vahid, and M. Mohsen, Types of solar cells and application. American Journal of optics and Photonics, 2015. 3(5): p. 94-113.

33. Noh, J.H., et al., Chemical management for colorful, efficient, and stable inorganic–organic hybrid nanostructured solar cells. Nano letters, 2013. 13(4): p. 1764-1769.

34. Dong, Q., et al., Electron-hole diffusion lengths> 175 μm in solution-grown CH3NH3PbI3 single crystals. Science, 2015. 347(6225): p. 967-970.

35. Xiao, Z., et al., Searching for promising new perovskite-based photovoltaic absorbers: the importance of electronic dimensionality. Materials Horizons, 2017. 4(2): p. 206-216.

36. Green, M.A., A. Ho-Baillie, and H.J. Snaith, The emergence of perovskite solar cells. Nature photonics, 2014. 8(7): p. 506-514.

37. Grätzel, M., The light and shade of perovskite solar cells. Nature materials, 2014. 13(9): p. 838-842.

38. Li, G., R. Zhu, and Y. Yang, Polymer solar cells. Nature photonics, 2012. 6(3): p. 153-161.

39. Kim, D.H., et al., 300% enhancement of carrier mobility in uniaxial-oriented perovskite films formed by topotactic-oriented attachment. Advanced Materials, 2017. 29(23): p. 1606831.

40. D'Innocenzo, V., et al., Tuning the light emission properties by band gap engineering in hybrid lead halide perovskite. Journal of the American Chemical Society, 2014. 136(51): p. 17730-17733.

41. Ameen, S., et al., Charge-transporting materials for perovskite solar cells, in Advances in Inorganic Chemistry. 2018, Elsevier. p. 185-246.

42. Kojima, A., et al., Organometal halide perovskites as visible-light sensitizers for photovoltaic cells. Journal of the american chemical society, 2009. 131(17): p. 6050-6051.

43. Liu, M., M.B. Johnston, and H.J. Snaith, Efficient planar heterojunction perovskite solar cells by vapour deposition. Nature, 2013. 501(7467): p. 395-398.

44. Nie, W., et al., High-efficiency solution-processed perovskite solar cells with millimeter-scale grains. Science, 2015. 347(6221): p. 522-525.

45. Fournier, O., et al., Interfacial tuning of hybrid halide triple cation perovskite solar cells with inorganic electron transport layer.

46. Noh, M.F.M., et al., The architecture of the electron transport layer for a perovskite solar cell. Journal of Materials Chemistry C, 2018. 6(4): p. 682-712.

47. Yang, G., et al., Tin oxide (SnO2) as effective electron selective layer material in hybrid organic–inorganic metal halide perovskite solar cells. Journal of energy chemistry, 2018. 27(4): p. 962-970.

48. Soh, M.F., et al., Incorporation of g-C3N4/Ag dopant in TiO2 as electron transport layer for organic solar cells. Materials Letters, 2019. 253: p. 117-120.

pg. 76

49. Dagar, J., et al., Efficient fully laser-patterned flexible perovskite modules and solar cells based on low-temperature solution-processed SnO 2/mesoporous-TiO 2 electron transport layers. Nano Research, 2018. 11: p. 2669-2681.

50. Sobayel, K., et al., A comprehensive defect study of tungsten disulfide (WS2) as electron transport layer in perovskite solar cells by numerical simulation. Results in Physics, 2019. 12: p. 1097-1103.

51. Zheng, X., et al., Defect passivation in hybrid perovskite solar cells using quaternary ammonium halide anions and cations. Nature Energy, 2017. 2(7): p. 1-9.

52. Singh, R., et al., Perovskite solar cells with an MoS 2 electron transport layer. Journal of Materials Chemistry A, 2019. 7(12): p. 7151-7158.

53. Kakavelakis, G., et al., 2D Transition Metal Dichalcogenides for Solution-Processed Organic and Perovskite Solar Cells. Two Dimensional Transition Metal Dichalcogenides: Synthesis, Properties, and Applications, 2019: p. 203-239.

54. Huang, P., et al., 21.7% efficiency achieved in planar n–i–p perovskite solar cells via interface engineering with water-soluble 2D TiS 2. Journal of Materials Chemistry A, 2019. 7(11): p. 6213-6219.

55. Xiao, S., et al., Atomic-layer soft plasma etching of MoS2. Scientific reports, 2016. 6(1): p. 19945.

56. Van Le, Q., J.-Y. Choi, and S.Y. Kim, Recent advances in the application of two-dimensional materials as charge transport layers in organic and perovskite solar cells. FlatChem, 2017. 2: p. 54-66.

57. Yang, G., et al., Recent progress in electron transport layers for efficient perovskite solar cells. Journal of Materials Chemistry A, 2016. 4(11): p. 3970-3990.

58. Luo, J., Y. Wang, and Q. Zhang, Progress in perovskite solar cells based on ZnO nanostructures. Solar Energy, 2018. 163: p. 289-306.

59. Ameri, M., et al., Self-assembled ZnO nanosheet-based spherical structure as photoanode in dye-sensitized solar cells. Journal of Electronic Materials, 2018. 47: p. 1993-1999.

60. Ahmadi, S.H., et al., Solvent selection for fabrication of low temperature ZnO electron transport layer in perovskite solar cells. Optical Materials, 2020. 106: p. 109977.

61. Miao, S., et al., Effect of oxygen vacancies in the electron transfer layer SiZnSnO on the performance of perovskite solar cells. Journal of Alloys and Compounds, 2020. 835: p. 155284.

62. Hussain, I., et al., Functional materials, device architecture, and flexibility of perovskite solar cell. Emergent Materials, 2018. 1: p. 133-154.

63. Lee, J.W., et al., High-efficiency perovskite solar cells based on the black polymorph of HC (NH2) 2PbI3. Advanced Materials, 2014. 26(29): p. 4991-4998.

64. Zhu, Q., et al., Compact layer free perovskite solar cells with a high-mobility hole-transporting layer. ACS applied materials & interfaces, 2016. 8(4): p. 2652-2657.

65. Yang, W.S., et al., High-performance photovoltaic perovskite layers fabricated through intramolecular exchange. Science, 2015. 348(6240): p. 1234-1237.

66. Aharon, S., et al., Depletion region effect of highly efficient hole conductor free CH 3 NH 3 PbI 3 perovskite solar cells. Physical Chemistry Chemical Physics, 2014. 16(22): p. 10512-10518.

67. Mei, A., et al., A hole-conductor–free, fully printable mesoscopic perovskite solar cell with high stability. science, 2014. 345(6194): p. 295-298.

68. Jeon, N.J., et al., Compositional engineering of perovskite materials for high-performance solar cells. Nature, 2015. 517(7535): p. 476-480.

69. Pellet, N., et al., Mixed-organic-cation Perovskite photovoltaics for enhanced solar-light harvesting. Angewandte Chemie International Edition, 2014. 53(12): p. 3151-3157.

70. Correa-Baena, J.-P., et al., The rapid evolution of highly efficient perovskite solar cells. Energy & Environmental Science, 2017. 10(3): p. 710-727.

71. Saliba, M., et al., Incorporation of rubidium cations into perovskite solar cells improves photovoltaic performance. Science, 2016. 354(6309): p. 206-209.

72. Saliba, M., et al., Cesium-containing triple cation perovskite solar cells: improved stability, reproducibility and high efficiency. Energy & environmental science, 2016. 9(6): p. 1989-1997.

73. Liu, C., et al., Highly efficient perovskite solar cells with substantial reduction of lead content. Scientific reports, 2016. 6(1): p. 35705.

74. Liu, Y., et al., Two-inch-sized perovskite CH3NH3PbX3 (X= Cl, Br, I) crystals: growth and characterization. Advanced materials, 2015. 27(35): p. 5176-5183.

75. Edri, E., et al., Chloride inclusion and hole transport material doping to improve methyl ammonium lead bromide perovskite-based high open-circuit voltage solar cells. The journal of physical chemistry letters, 2014. 5(3): p. 429-433.

76. Suarez, B., et al., Recombination study of combined halides (Cl, Br, I) perovskite solar cells. The journal of physical chemistry letters, 2014. 5(10): p. 1628-1635.

77. Lee, J.W., et al., Formamidinium and cesium hybridization for photo-and moisture-stable perovskite solar cell. Advanced Energy Materials, 2015. 5(20): p. 1501310.

78. Lee, M.M., et al., Efficient hybrid solar cells based on meso-superstructured organometal halide perovskites. Science, 2012. 338(6107): p. 643-647.

79. Jacobsson, T.J., et al., Exploration of the compositional space for mixed lead halogen perovskites for high efficiency solar cells. Energy & Environmental Science, 2016. 9(5): p. 1706-1724.

80. Noel, N.K., et al., Lead-free organic–inorganic tin halide perovskites for photovoltaic applications. Energy & Environmental Science, 2014. 7(9): p. 3061-3068.

81. Yin, W.-J., Y. Yan, and S.-H. Wei, Anomalous alloy properties in mixed halide perovskites. The journal of physical chemistry letters, 2014. 5(21): p. 3625-3631.

82. Anaraki, E.H., et al., Highly efficient and stable planar perovskite solar cells by solution-processed tin oxide. Energy & Environmental Science, 2016. 9(10): p. 3128-3134.

83. Harikesh, P.C., et al., Rb as an alternative cation for templating inorganic lead-free perovskites for solution processed photovoltaics. Chemistry of Materials, 2016. 28(20): p. 7496-7504.

84. Krishnamoorthy, T., et al., Lead-free germanium iodide perovskite materials for photovoltaic applications. Journal of Materials Chemistry A, 2015. 3(47): p. 23829-23832.

85. Chang, C.-Y., et al., Tuning perovskite morphology by polymer additive for high efficiency solar cell. ACS applied materials & interfaces, 2015. 7(8): p. 4955-4961.

86. Qian, J., B. Xu, and W. Tian, A comprehensive theoretical study of halide perovskites ABX3. Organic Electronics, 2016. 37: p. 61-73.

87. Conings, B., et al., An easy-to-fabricate low-temperature TiO2 electron collection layer for high efficiency planar heterojunction perovskite solar cells. APL Materials, 2014. 2(8): p. 081505.

88. Cui, X.-P., et al., Cupric bromide hybrid perovskite heterojunction solar cells. Synthetic metals, 2015. 209: p. 247-250.

89. Kopacic, I., et al., Enhanced performance of germanium halide perovskite solar cells through compositional engineering. ACS Applied Energy Materials, 2018. 1(2): p. 343-347.

90. Shai, X., et al., Efficient planar perovskite solar cells using halide Sr-substituted Pb perovskite. Nano Energy, 2017. 36: p. 213-222.

91. Im, J.-H., H.-S. Kim, and N.-G. Park, Morphology-photovoltaic property correlation in perovskite solar cells: One-step versus two-step deposition of CH3NH3PbI3. Apl Materials, 2014. 2(8): p. 081510.

92. Razza, S., et al., Perovskite solar cells and large area modules (100 cm2) based on an air flow-assisted PbI2 blade coating deposition process. Journal of Power Sources, 2015. 277: p. 286-291.

93. Adnan, M. and J.K. Lee, all sequential dip-coating processed perovskite layers from an aqueous lead precursor for high efficiency perovskite solar cells. Scientific reports, 2018. 8(1): p. 1-10.

94. Kim, J.-E., et al., Slot die coated planar perovskite solar cells via blowing and heating assisted one step deposition. Solar Energy Materials and Solar Cells, 2018. 179: p. 80-86.

95. Habibi, M., M.-R. Ahmadian-Yazdi, and M. Eslamian, Optimization of spray coating for the fabrication of sequentially deposited planar perovskite solar cells. Journal of Photonics for Energy, 2017. 7(2): p. 022003-022003.

96. Mathies, F., et al., Inkjet-printed triple cation perovskite solar cells. ACS Applied Energy Materials, 2018. 1(5): p. 1834-1839.

97. Ono, L.K., et al., Organometal halide perovskite thin films and solar cells by vapor deposition. Journal of Materials Chemistry A, 2016. 4(18): p. 6693-6713.

98. Tzounis, L., et al., Perovskite solar cells from small scale spin coating process towards roll-to-roll printing: Optical and morphological studies. Materials Today: Proceedings, 2017. 4(4): p. 5082-5089.

99. Deng, Y., et al., Scalable fabrication of efficient organolead trihalide perovskite solar cells with doctor-bladed active layers. Energy & Environmental Science, 2015. 8(5): p. 1544-1550.

100. Song, J., et al., Low-temperature SnO 2-based electron selective contact for efficient and stable perovskite solar cells. Journal of Materials Chemistry A, 2015. 3(20): p. 10837-10844.

101. Cotella, G., et al., One-step deposition by slot-die coating of mixed lead halide perovskite for photovoltaic applications. Solar Energy Materials and Solar Cells, 2017. 159: p. 362-369.

102. Marinova, N., S. Valero, and J.L. Delgado, Organic and perovskite solar cells: Working principles, materials and interfaces. Journal of colloid and interface science, 2017. 488: p. 373-389.

103. Chen, B., et al., Origin of J–V hysteresis in perovskite solar cells. The journal of physical chemistry letters, 2016. 7(5): p. 905-917.

104. Wang, Z., et al., Solution processed Nb2O5 electrodes for high efficient ultraviolet light stable planar perovskite solar cells. ACS Sustainable Chemistry & Engineering, 2019. 7(7): p. 7421-7429.

105. Yuan, Z., et al., Unveiling the synergistic effect of precursor stoichiometry and interfacial reactions for perovskite light-emitting diodes. Nature communications, 2019. 10(1): p. 2818.

106. Li, X., et al., Low-temperature solution-processed ZnSe electron transport layer for efficient planar perovskite solar cells with negligible hysteresis and improved photostability. ACS nano, 2018. 12(6): p. 5605-5614.

107. Hong, W.-C., et al., MgZnO high voltage thin film transistors on glass for inverters in building integrated photovoltaics. Scientific reports, 2016. 6(1): p. 34169.

108. Teimouri, R., et al., Synthesizing Li doped TiO2 electron transport layers for highly efficient planar perovskite solar cell. Superlattices and Microstructures, 2020. 145: p. 106627.

109. Yang, Z., et al., Flexible MAPbI3 perovskite solar cells with the high efficiency of 16.11% by low-temperature synthesis of compact anatase TiO2 film. Journal of Alloys and Compounds, 2021. 854: p. 155488.

110. Zhang, B., et al., Applying neoteric MgTiO3-coated TiO2 nanoparticulate films as scaffold layers in perovskite solar cells based on carbon counter electrode for retarding charge recombination. Electrochimica Acta, 2020. 338: p. 135884.

111. Yin, P., et al., Controlling the mechanism of excitonic splitting in In2O3 nanocrystals by carrier delocalization. ACS nano, 2018. 12(11): p. 11211-11218.

112. Zhang, X., et al., Stable and efficient air-processed perovskite solar cells employing low-temperature processed compact In2O3 thin films as electron transport materials. Journal of Alloys and Compounds, 2020. 836: p. 155460.

113. Epifani, M., et al., Solution synthesis of thin films in the SnO2− In2O3 system: a case study of the mixing of sol− gel and metal-organic solution processes. Chemistry of materials, 2006. 18(3): p. 840-846.

114. Tseng, C.-C., et al., Cu2O-HTM/SiO2-ETM assisted for synthesis engineering improving efficiency and stability with heterojunction planar perovskite thin-film solar cells. Solar Energy, 2020. 204: p. 270-279.

115. Habibi, M., et al., Progress in emerging solution-processed thin film solar cells–Part II: Perovskite solar cells. Renewable and Sustainable Energy Reviews, 2016. 62: p. 1012-1031.

116. Park, N.-G., Perovskite solar cells: an emerging photovoltaic technology. Materials today, 2015. 18(2): p. 65-72.

117. Zhong, M., et al., Enhanced efficiency and stability of perovskite solar cell by adding polymer mixture in perovskite photoactive layer. Journal of Alloys and Compounds, 2021. 864: p. 158793.

118. Shen, K., et al., Emerging characterizing techniques in the fine structure observation of metal halide perovskite crystal. Crystals, 2018. 8(6): p. 232.

119. Forrester, W. and R. Hinde, Crystal structure of barium titanate. Nature, 1945. 156(3954): p. 177-177.

120. Jena, A.K., A. Kulkarni, and T. Miyasaka, Halide perovskite photovoltaics: background, status, and future prospects. Chemical reviews, 2019. 119(5): p. 3036-3103.

121. Chen, J., et al., Recent progress in stabilizing hybrid perovskites for solar cell applications. Journal of Power Sources, 2017. 355: p. 98-133.

122. Snaith, H.J., et al., Anomalous hysteresis in perovskite solar cells. The journal of physical chemistry letters, 2014. 5(9): p. 1511-1515.

123. Tonui, P., et al., Perovskites photovoltaic solar cells: An overview of current status. Renewable and Sustainable Energy Reviews, 2018. 91: p. 1025-1044.

124. Jung, H.S. and N.G. Park, Perovskite solar cells: from materials to devices. small, 2015. 11(1): p. 10-25.

125. Tai, Q., et al., Recent advances toward efficient and stable tin-based perovskite solar cells. EcoMat, 2019. 1(1): p. e12004.

126. Giustino, F. and H.J. Snaith, Toward lead-free perovskite solar cells. ACS Energy Letters, 2016. 1(6): p. 1233-1240.

127. Ning, W. and F. Gao, Structural and functional diversity in lead-free halide perovskite materials. Advanced Materials, 2019. 31(22): p. 1900326.

128. Ke, W., C.C. Stoumpos, and M.G. Kanatzidis, "Unleaded" perovskites: status quo and future prospects of tin-based perovskite solar cells. Advanced Materials, 2019. 31(47): p. 1803230.

129. Konstantakou, M. and T. Stergiopoulos, A critical review on tin halide perovskite solar cells. Journal of Materials Chemistry A, 2017. 5(23): p. 11518-11549.

130. Hao, F., et al., Lead-free solid-state organic–inorganic halide perovskite solar cells. Nature photonics, 2014. 8(6): p. 489-494.

131. Yokoyama, T., et al., Overcoming short-circuit in lead-free CH3NH3SnI3 perovskite solar cells via kinetically controlled gas–solid reaction film fabrication process. The journal of physical chemistry letters, 2016. 7(5): p. 776-782.

132. Song, T.-B., et al., Importance of reducing vapor atmosphere in the fabrication of tin-based perovskite solar cells. Journal of the American Chemical Society, 2017. 139(2): p. 836-842.

133. Kumar, M.H., et al., Lead-free halide perovskite solar cells with high photocurrents realized through vacancy modulation. Advanced Materials, 2014. 26(41): p. 7122-7127.

134. Liu, X., et al., Improving the performance of inverted formamidinium tin iodide perovskite solar cells by reducing the energy-level mismatch. ACS Energy Letters, 2018. 3(5): p. 1116-1121.

135. Lee, S.J., et al., Fabrication of efficient formamidinium tin iodide perovskite solar cells through SnF2–pyrazine complex. Journal of the American Chemical Society, 2016. 138(12): p. 3974-3977.

136. Liao, W., et al., Lead-free inverted planar formamidinium tin triiodide perovskite solar cells achieving power conversion efficiencies up to 6.22%. Advanced Materials, 2016. 28(42): p. 9333-9340.

137. Ke, W., et al., Enhanced photovoltaic performance and stability with a new type of hollow 3D perovskite {en} FASnI3. Science advances, 2017. 3(8): p. e1701293.

138. Yang, Z., et al., SnO2-C60 Pyrrolidine Tris-Acid (CPTA) as the Electron Transport Layer for Highly Efficient and Stable Planar Sn-Based Perovskite Solar Cells. Advanced Functional Materials, 2019. 29(42): p. 1903621.

139. Liu, X., et al., Solvent engineering improves efficiency of lead-free tin-based hybrid perovskite solar cells beyond 9%. ACS Energy Letters, 2018. 3(11): p. 2701-2707.

140. Wang, F., et al., 2D-quasi-2D-3D hierarchy structure for tin perovskite solar cells with enhanced efficiency and stability. Joule, 2018. 2(12): p. 2732-2743.

141. Jokar, E., et al., Robust tin-based perovskite solar cells with hybrid organic cations to attain efficiency approaching 10%. Advanced materials, 2019. 31(2): p. 1804835.

142. Kamarudin, M.A., et al., Suppression of charge carrier recombination in lead-free tin halide perovskite via Lewis base post-treatment. The journal of physical chemistry letters, 2019. 10(17): p. 5277-5283.

143. Li, W., et al., Addictive-assisted construction of all-inorganic CsSnIBr 2 mesoscopic perovskite solar cells with superior thermal stability up to 473 K. Journal of materials chemistry A, 2016. 4(43): p. 17104-17110.

144. Tai, Q., et al., Antioxidant grain passivation for air-stable tin-based perovskite solar cells. Angewandte Chemie International Edition, 2019. 58(3): p. 806-810.

145. Kayesh, M.E., et al., Enhanced photovoltaic performance of FASnI3-based perovskite solar cells with hydrazinium chloride coadditive. ACS Energy Letters, 2018. 3(7): p. 1584-1589.

146. Li, F., et al., Trihydrazine Dihydriodide-Assisted Fabrication of Efficient Formamidinium Tin Iodide Perovskite Solar Cells. Solar RRL, 2019. 3(9): p. 1900285.

147. Gu, F., et al., Improving performance of lead-free formamidinium tin triiodide perovskite solar cells by tin source purification. Solar RRL, 2018. 2(10): p. 1800136.

148. Gu, F., et al., Lead-free tin-based perovskite solar cells: strategies toward high performance. Solar Rrl, 2019. 3(9): p. 1900213.

149. Chen, M., et al., Highly stable and efficient all-inorganic lead-free perovskite solar cells with native-oxide passivation. Nature communications, 2019. 10(1): p. 16.

150. Du, J., et al., Enhanced efficiency and stability of planar perovskite solar cells by introducing amino acid to SnO2/perovskite interface. Journal of Power Sources, 2020. 455: p. 227974.

151. Sun, C., et al., Ternary oxide BaSnO3 nanoparticles as an efficient electron-transporting layer for planar perovskite solar cells. Journal of Alloys and Compounds, 2017. 722: p. 196-206.

152. Bera, A., et al., Perovskite oxide SrTiO3 as an efficient electron transporter for hybrid perovskite solar cells. The Journal of Physical Chemistry C, 2014. 118(49): p. 28494-28501.

153. Zhang, M., et al., Simple route to interconnected, hierarchically structured, porous Zn2SnO4 nanospheres as electron transport layer for efficient perovskite solar cells. Nano Energy, 2020. 71: p. 104620.

154. Oh, L.S., et al., Zn2SnO4-based photoelectrodes for organolead halide perovskite solar cells. The Journal of Physical Chemistry C, 2014. 118(40): p. 22991-22994.

155. Shin, S.S., et al., High-performance flexible perovskite solar cells exploiting Zn2SnO4 prepared in solution below 100° C. Nature communications, 2015. 6(1): p. 7410.

156. Jung, K., et al., Highly efficient amorphous Zn2SnO4 electron-selective layers yielding over 20% efficiency in FAMAPbI3-based planar solar cells. ACS Energy Letters, 2018. 3(10): p. 2410-2417.

157. Zheng, M., et al., Mesostructured perovskite solar cells based on Zn2SnO4 single crystal mesoporous layer with efficiency of 18.32%. Journal of Alloys and Compounds, 2020. 823: p. 153730.

158. Jeon, N.J., et al., A fluorene-terminated hole-transporting material for highly efficient and stable perovskite solar cells. Nature Energy, 2018. 3(8): p. 682-689.

159. Zhang, L., et al., Intensive exposure of functional rings of a polymeric hole-transporting material enables efficient perovskite solar cells. Advanced Materials, 2018. 30(39): p. 1804028.

160. Wang, M.Z., et al., PbTiO3 as Electron-Selective Layer for High-Efficiency Perovskite Solar Cells: Enhanced Electron Extraction via Tunable Ferroelectric Polarization. Advanced Functional Materials, 2019. 29(1): p. 1806427.

161. You, J., et al., Improved air stability of perovskite solar cells via solution-processed metal oxide transport layers. Nature nanotechnology, 2016. 11(1): p. 75-81.

162. Zheng, S., et al., Materials and structures for the electron transport layer of efficient and stable perovskite solar cells. Science China Chemistry, 2019. 62: p. 800-809.

163. Cheng, N., et al., Application of mesoporous SiO2 layer as an insulating layer in high performance hole transport material free CH3NH3PbI3 perovskite solar cells. Journal of Power Sources, 2016. 321: p. 71-75.

164. Bharti, B., et al., Formation of oxygen vacancies and Ti3+ state in TiO2 thin film and enhanced optical properties by air plasma treatment. Scientific reports, 2016. 6(1): p. 32355.

165. Yang, Y., et al., An ultrathin ferroelectric perovskite oxide layer for high-performance hole transport material free carbon based halide perovskite solar cells. Advanced Functional Materials, 2019. 29(1): p. 1806506.

166. Tao, H., et al., TiO2@ PbTiO3 core-shell nanoparticles as mesoporous layer to improve electron transport performance in carbon-based perovskite solar cells. Materials Chemistry and Physics, 2020. 254: p. 123436.

167. Du, Y., et al., Precursor engineering for performance enhancement of hole-transport-layer-free carbon-based MAPbBr3 perovskite solar cells. Journal of Alloys and Compounds, 2020. 832: p. 154902.

168. Song, J., et al., Quantum dot light-emitting diodes based on inorganic perovskite cesium lead halides (CsPbX3). Advanced materials, 2015. 27(44): p. 7162-7167.

169. Gao, Y., et al., CsPbBr3 perovskite nanoparticles as additive for environmentally stable perovskite solar cells with 20.46% efficiency. Nano Energy, 2019. 59: p. 517-526.

170. Yantara, N., et al., Inorganic halide perovskites for efficient light-emitting diodes. The journal of physical chemistry letters, 2015. 6(21): p. 4360-4364.

171. Ma, Q., et al., Hole transport layer free inorganic CsPbIBr2 perovskite solar cell by dual source thermal evaporation. Advanced energy materials, 2016. 6(7): p. 1502202.

172. Zhu, W., et al., Aged precursor solution toward low-temperature fabrication of efficient carbon-based all-inorganic planar CsPbIBr2 perovskite solar cells. ACS Applied Energy Materials, 2018. 1(9): p. 4991-4997.

173. Wang, G., et al., Optimizing the substrate pre-heating and post-annealing temperatures for fabricating high-performance carbon-based CsPbIBr2 inorganic perovskite solar cells. Electrochimica Acta, 2020. 349: p. 136354.

174. Pei, Y., et al., BiBr3 as an additive in CsPbBr3 for carbon-based all-inorganic perovskite solar cell. Journal of Alloys and Compounds, 2020. 835: p. 155283.

175. Ding, J., et al., Alloy-Controlled Work Function for Enhanced Charge Extraction in All-Inorganic CsPbBr3 Perovskite Solar Cells. ChemSusChem, 2018. 11(9): p. 1432-1437.

176. Zong, Z., et al., Boosted hole extraction in all-inorganic CsPbBr3 perovskite solar cells by interface engineering using MoO2/N-doped carbon nanospheres composite. Solar Energy Materials and Solar Cells, 2020. 209: p. 110460.

177. Niu, T., et al., Stable high-performance perovskite solar cells via grain boundary passivation. Advanced Materials, 2018. 30(16): p. 1706576.

178. Litvin, A.P., et al., Carbon-based interlayers in perovskite solar cells. Renewable and Sustainable Energy Reviews, 2020. 124: p. 109774.

179. Liu, J., et al., Hole and electron extraction layers based on graphene oxide derivatives for high-performance bulk heterojunction solar cells. Advanced Materials, 2012. 24(17): p. 2228-2233.

180. Mahmoudi, T., et al., Highly conductive and dispersible graphene and its application in P3HT-based solar cells. Chemical Communications, 2014. 50(63): p. 8705-8708.

181. Agresti, A., et al., Efficiency and stability enhancement in perovskite solar cells by inserting lithium-neutralized graphene oxide as electron transporting layer. Advanced Functional Materials, 2016. 26(16): p. 2686-2694.

182. Liu, T., et al., Fine-tuning optical and electronic properties of graphene oxide for highly efficient perovskite solar cells. Nanoscale, 2015. 7(24): p. 10708-10718.

183. Liu, J., Y. Xue, and L. Dai, Sulfated graphene oxide as a hole-extraction layer in high-performance polymer solar cells. The journal of physical chemistry letters, 2012. 3(14): p. 1928-1933.

184. Kim, J.M., et al., Use of AuCl3-doped graphene as a protecting layer for enhancing the stabilities of inverted perovskite solar cells. Applied Surface Science, 2018. 455: p. 1131-1136.

185. Yun, J.M., et al., Solution-processable reduced graphene oxide as a novel alternative to PEDOT: PSS hole transport layers for highly efficient and stable polymer solar cells. Advanced Materials, 2011. 23(42): p. 4923-4928.

186. Choi, E.-S., et al., Metal chloride-treated graphene oxide to produce high-performance polymer solar cells. Applied Physics Letters, 2015. 107(2): p. 67_1.

187. Mahmoudi, T., et al., Efficient bulk heterojunction hybrid solar cells with graphene-silver nanoparticles composite synthesized by microwave-assisted reduction. Nano Energy, 2016. 28: p. 179-187.

188. Kim, S.-H., et al., Fluorine-functionalized and simultaneously reduced graphene oxide as a novel hole transporting layer for highly efficient and stable organic photovoltaic cells. Nanoscale, 2014. 6(13): p. 7183-7187.

189. Yang, D., et al., Chemically modified graphene oxides as a hole transport layer in organic solar cells. Chemical Communications, 2012. 48(65): p. 8078-8080.

190. Yang, D., et al., Work-function-tunable chlorinated graphene oxide as an anode interface layer in high-efficiency polymer solar cells. Advanced Energy Materials, 2014. 4(15): p. 1400591.

191. Stratakis, E., et al., Improving the efficiency of organic photovoltaics by tuning the work function of graphene oxide hole transporting layers. Nanoscale, 2014. 6(12): p. 6925-6931.

192. Feng, S., et al., High-performance perovskite solar cells engineered by an ammonia modified graphene oxide interfacial layer. ACS applied materials & interfaces, 2016. 8(23): p. 14503-14512.

193. Yang, Y., et al., High performance carbon-based planar perovskite solar cells by hot-pressing approach. Solar Energy Materials and Solar Cells, 2020. 210: p. 110517.

194. He, R., et al., Carbon-based perovskite solar cells: from single-junction to modules. Carbon Energy, 2019. 1(1): p. 109-123.

195. Im, J.-H., et al., 6.5% efficient perovskite quantum-dot-sensitized solar cell. Nanoscale, 2011. 3(10): p. 4088-4093.

196. Wu, Z., et al., Highly efficient and stable perovskite solar cells via modification of energy levels at the perovskite/carbon electrode interface. Advanced Materials, 2019. 31(11): p. 1804284.

197. KantháSiram, R.B., Hybrid organic nanocrystal/carbon nanotube film electrodes for air-and photo-stable perovskite photovoltaics. Nanoscale, 2019. 11(8): p. 3733-3740.

198. Raminafshar, C., et al., Carbon based perovskite solar cells constructed by screen-printed components. Electrochimica Acta, 2018. 276: p. 261-267.

199. Yoon, J., et al., Superflexible, high-efficiency perovskite solar cells utilizing graphene electrodes: towards future foldable power sources. Energy & Environmental Science, 2017. 10(1): p. 337-345.

200. Jang, C.W., J.M. Kim, and S.-H. Choi, Lamination-produced semi-transparent/flexible perovskite solar cells with doped-graphene anode and cathode. Journal of Alloys and Compounds, 2019. 775: p. 905-911.

201. Zhang, H., et al., Self-adhesive macroporous carbon electrodes for efficient and stable perovskite solar cells. Advanced Functional Materials, 2018. 28(39): p. 1802985.

202. Mashhoun, S., et al., Resolving a critical instability in perovskite solar cells by designing a scalable and printable carbon based electrode-interface architecture. Advanced Energy Materials, 2018. 8(31): p. 1802085.

203. Ryu, J., et al., Paintable carbon-based perovskite solar cells with engineered perovskite/carbon interface using carbon nanotubes dripping method. Small, 2017. 13(38): p. 1701225.

204. Jiang, P., et al., Fully printable perovskite solar cells with highly-conductive, low-temperature, perovskite-compatible carbon electrode. Carbon, 2018. 129: p. 830-836.

205. Zhang, L., et al., The effect of carbon counter electrodes on fully printable mesoscopic perovskite solar cells. Journal of Materials Chemistry A, 2015. 3(17): p. 9165-9170.

206. Chu, L., et al., Boosting efficiency of hole conductor-free perovskite solar cells by incorporating p-type NiO nanoparticles into carbon electrodes. Solar Energy Materials and Solar Cells, 2018. 178: p. 164-169.

207. Meng, F., et al., Ultra-low-cost coal-based carbon electrodes with seamless interfacial contact for effective sandwich-structured perovskite solar cells. Carbon, 2019. 145: p. 290-296.

208. Wei, W., et al., Potassium-chemical synthesis of 3D graphene from CO 2 and its excellent performance in HTM-free perovskite solar cells. Journal of Materials Chemistry A, 2017. 5(17): p. 7749-7752.

209. Matteocci, F., et al., Encapsulation for long-term stability enhancement of perovskite solar cells. Nano Energy, 2016. 30: p. 162-172.

210. Chang, C.-Y., W.-K. Huang, and Y.-C. Chang, Highly-efficient and long-term stable perovskite solar cells enabled by a cross-linkable n-doped hybrid cathode interfacial layer. Chemistry of Materials, 2016. 28(17): p. 6305-6312.

211. Chiang, C.H. and C.G. Wu, Film grain-size related long-term stability of inverted perovskite solar cells. ChemSusChem, 2016. 9(18): p. 2666-2672.

212. Wang, Q., et al., Scaling behavior of moisture-induced grain degradation in polycrystalline hybrid perovskite thin films. Energy & Environmental Science, 2017. 10(2): p. 516-522.

213. Qiu, L., et al., Engineering interface structure to improve efficiency and stability of organometal halide perovskite solar cells. The Journal of Physical Chemistry B, 2017. 122(2): p. 511-520.

214. Zhang, L., et al., Interactions between molecules and perovskites in halide perovskite solar cells. Solar Energy Materials and Solar Cells, 2018. 175: p. 1-19.

215. Lira-Cantú, M., Perovskite solar cells: Stability lies at interfaces. Nature Energy, 2017. 2(7): p. 1-3.

216. Yun, J.S., et al., Humidity-induced degradation via grain boundaries of HC (NH2) 2PbI3 planar perovskite solar cells. Advanced Functional Materials, 2018. 28(11): p. 1705363.

217. Peng, J., et al., A universal double-side passivation for high open-circuit voltage in perovskite solar cells: role of carbonyl groups in poly (methyl methacrylate). Advanced Energy Materials, 2018. 8(30): p. 1801208.

218. Zhang, F., et al., Over 20% PCE perovskite solar cells with superior stability achieved by novel and low-cost hole-transporting materials. Nano Energy, 2017. 41: p. 469-475.

219. Zhao, Y.-C., et al., Quantification of light-enhanced ionic transport in lead iodide perovskite thin films and its solar cell applications. Light: Science & Applications, 2017. 6(5): p. e16243-e16243.

220. Zhou, P., et al., Nonconjugated polymer poly (vinylpyrrolidone) as an efficient interlayer promoting electron transport for perovskite solar cells. ACS applied materials & interfaces, 2017. 9(38): p. 32957-32964.

221. Dong, Q., et al., Easily accessible polymer additives for tuning the crystal-growth of perovskite thin-films for highly efficient solar cells. Nanoscale, 2016. 8(10): p. 5552-5558.

222. Isakova, A. and P.D. Topham, Polymer strategies in perovskite solar cells. Journal of Polymer Science Part B: Polymer Physics, 2017. 55(7): p. 549-568.

223. Astruc, D., E. Boisselier, and C. Ornelas, Dendrimers designed for functions: from physical, photophysical, and supramolecular properties to applications in sensing, catalysis, molecular electronics, photonics, and nanomedicine. Chemical reviews, 2010. 110(4): p. 1857-1959.

224. Du, Y., et al., Dendritic PAMAM polymers for strong perovskite intergranular interaction enhancing power conversion efficiency and stability of perovskite solar cells. Electrochimica Acta, 2020. 349: p. 136387.

225. Kang, J.H., et al., Cationic polyelectrolytes as convenient electron extraction layers in perovskite solar cells. Dyes and Pigments, 2020. 182: p. 108634.

226. Magomedov, A., et al., Self-assembled hole transporting monolayer for highly efficient perovskite solar cells. Advanced energy materials, 2018. 8(32): p. 1801892.

227. Xu, L., et al., Efficient, high yield perovskite/fullerene planar-heterojunction solar cells via one-step spin-coating processing. RSC advances, 2016. 6(54): p. 48449-48454.

228. Syed, A.A., et al., A sodium citrate-modified-PEDOT: PSS hole transporting layer for performance enhancement in inverted planar perovskite solar cells. Journal of Materials Chemistry C, 2019. 7(18): p. 5260-5266.

229. Tang, H., et al., Energy Level Tuning of PEDOT: PSS for High Performance Tin-Lead Mixed Perovskite Solar Cells. Solar RRL, 2019. 3(2): p. 1800256.

230. Chen, K., et al., Charge-carrier balance for highly efficient inverted planar heterojunction perovskite solar cells. Advanced materials, 2016. 28(48): p. 10718-10724.

231. Xu, L., et al., Improving the efficiency and stability of inverted perovskite solar cells by CuSCN-doped PEDOT: PSS. Solar Energy Materials and Solar Cells, 2020. 206: p. 110316.

232. Ma, S., et al., Efficient and flexible solar cells with improved stability through incorporation of a multifunctional small molecule at PEDOT: PSS/perovskite interface. Solar Energy Materials and Solar Cells, 2020. 208: p. 110379.

233. Song, Z., et al., Pathways toward high-performance perovskite solar cells: review of recent advances in organo-metal halide perovskites for photovoltaic applications. Journal of photonics for energy, 2016. 6(2): p. 022001-022001.

234. Elumalai, N.K., et al., Perovskite solar cells: progress and advancements. Energies, 2016. 9(11): p. 861.

235. Chen, L., et al., Fabrication and properties of high-efficiency perovskite/PCBM organic solar cells. Nanoscale Res Lett 10: 312. 2015.

236. Zhang, J., et al., Binary solvent engineering for high-performance two-dimensional perovskite solar cells. ACS Sustainable Chemistry & Engineering, 2019. 7(3): p. 3487-3495.

237. Silva Filho, J.M.C.d., V.A. Ermakov, and F.C. Marques, Perovskite thin film synthesised from sputtered lead sulphide. Scientific Reports, 2018. 8(1): p. 1563.

238. Torabi, N., et al., Progress and challenges in perovskite photovoltaics from single-to multi-junction cells. Materials Today Energy, 2019. 12: p. 70-94.

239. Burschka, J., et al., Sequential deposition as a route to high-performance perovskite-sensitized solar cells. Nature, 2013. 499(7458): p. 316-319.

240. Zhao, Q., et al., Achieving efficient inverted planar perovskite solar cells with nondoped PTAA as a hole transport layer. Organic Electronics, 2019. 71: p. 106-112.

241. Li, W., et al., Controllable grain morphology of perovskite absorber film by molecular self-assembly toward efficient solar cell exceeding 17%. Journal of the American Chemical Society, 2015. 137(32): p. 10399-10405.

242. Tafazoli, S., et al., The role of a vapor-assisted solution process on tailoring the chemical composition and morphology of mixed-halide perovskite solar cells. CrystEngComm, 2018. 20(31): p. 4428-4435.

243. Zimmermann, I., et al., Sequentially Slot-Die-Coated Perovskite for Efficient and Scalable Solar Cells. Advanced Materials Interfaces, 2021. 8(18): p. 2100743.

244. Khadka, D.B., et al., Enhancement in efficiency and optoelectronic quality of perovskite thin films annealed in MACl vapor. Sustainable Energy & Fuels, 2017. 1(4): p. 755-766.

245. Chen, Y., et al., Large-area perovskite solar cells–a review of recent progress and issues. RSC advances, 2018. 8(19): p. 10489-10508.

246. Liang, G., et al., Highly uniform large-area (100 cm^2) perovskite CH3NH3PbI3 thin-films prepared by single-source thermal evaporation. Coatings, 2018. 8(8): p. 256.

247. NREL, N., Research cell efficiency records. 2019.